Current limitations of molecular dynamic simulations as probes of thermo-physical behavior of silicate melts

Revision 1

Jean-Philippe Harvey[1,*] and Paul D. Asimow[1]

[1]Division of Geological and Planetary Sciences, California Institute of Technology, Pasadena CA 91125 USA

*jpharvey@caltech.edu

Abstract

Molecular dynamic simulations offer promise as an essential tool, complementary to experiments, for expanding the reach of computational thermodynamics in igneous petrology by evaluating excess thermodynamic properties of multicomponent silicate melts. However, we present evidence suggesting that current practices in simulation may not achieve the precision needed to predict complex phase equilibria relevant to modeling the Earth's interior evolution. We highlight the importance of quantification of the chemical short range order in terms of cation-cation pairs in the melt and its impact on different kinetic aspects of molecular dynamic simulations. We analyze published molecular dynamic simulation studies of silicate melts in order to identify specific criteria and best practices for achieving and demonstrating equilibrium and producing accurate results. Finally, we propose a list of experimental and numerical investigations that need to be performed in the future to ensure full consistency between these two approaches in order to reduce the gap in our fundamental understanding of silicate melts between the atomic level and the macroscopic scale.

Always consult and cite the final, published document. See http://www.minsocam.org or GeoscienceWorld

Keywords: molecular dynamics, ab initio calculations, classical thermodynamics, silicate melts

1. Introduction

Our ability to describe the range of evolutionary pathways for terrestrial planets and to identify, through interpretation of available data, the particular pathway that the Earth followed depends on our understanding of the thermo-physical properties of Earth materials under a wide range of conditions. Multi-component liquid solutions of oxides, metals and silicates, in particular, are the defining materials of magmatic processes that have driven chemical differentiation throughout planetary history and that continue to modulate ongoing dynamic processes and natural volcanic hazards. Questions whose answers depend on such liquid properties include (but are not limited to): temperature and heat flow profiles across the earth's mantle over time (Davies, 2006, 2008); bulk chemical composition and both radial and lateral heterogeneity of mantle and crust (Solomatov and Stevenson, 1993); and evolution of oxidation state and the speciation and outgassing (and ingassing) of volatile components, an essential part of the story of Earth's habitability over time (Dasgupta and Hirschmann, 2006; Hirschmann, 2006).

In turn, the properties of melts and partial melts that must be predicted accurately as functions of temperature (T), pressure (P) or volume (V), and composition include elastic and thermodynamic quantities as well as dynamic transport properties such as viscosity, thermal conductivity and chemical diffusivities (Stixrude et al. 2009). The densities of silicate melts, solids and glasses define the driving forces by which gravity leads to physical flow and differential transport of phases (Agee, 1998; de Koker et al. 2013; Lange and Carmichael, 1987; McKenzie, 1984, 1985; Sparks and Parmentier, 1991; Stolper et al. 1981). Standard-state thermodynamic quantities and activity-composition relationships govern phase equilibria and provide the driving forces for chemical transport and differential transport of species within phases (Fei et al. 1990; Ghiorso,

Always consult and cite the final, published document. See http://www.minsocam.org or GeoscienceWorld

1985). Viscosity of melts controls many aspects of magma transport and chemical evolution of magmas (Clemens and Petford, 1999; Dingwell, 1996, 1998; Vetere et al. 2008; Whittington et al. 2009), although texture of multiphase aggregates is important as well (Faul et al. 1994; von Bargen and Waff, 1986). Chemical and self-diffusivity of various species lead to stable isotope fractionation (Lacks et al. 2012; Lundstrom et al. 2005; Richter et al. 2003) and are often rate-limiting in crystal growth in igneous rocks (Faul and Scott, 2006) and more generally in the achievement of thermodynamic equilibrium (Lesher, 2010; Liang, 2003).

The behavior and distribution of silicate liquids can be addressed near the surface and in both the present and the past through collection and analysis of igneous rocks (Klein and Langmuir, 1987; Lee et al. 2009; Lehnert et al. 2000; Niu et al. 2011; Plank and Langmuir, 1988), whereas the current distribution of melts at depth can be inferred from seismological (Forsyth, 1996; Karato and Jung, 1998; Lay et al. 2004; Williams and Garnero, 1996) or magnetotelluric (Evans et al. 2005; Matsuno et al. 2012) measurements. However, many melting-related phenomena occur at extreme P and T, where observational and even experimental data are available only at sparsely sampled compositions and (P, T) or are lacking altogether. This creates an obvious need for theoretical or computational approaches in order to construct and calibrate a successful, general model of liquids, applicable to all relevant compositions and conditions and capable of predicting all thermodynamic and kinetic properties. The question is how to construct such a model. We propose that major progress can be achieved through a combination of approaches from Earth science and from engineering thermodynamics that have yet to be brought together.

1.1 The goal

An ultimate strategy to self-consistently represent and predict the thermo-physical behavior of silicate melts should link together the internal energy (U), the structure and the equilibrium

Always consult and cite the final, published document. See http://www.minsocam.org or GeoscienceWorld

molar volume in order to provide a predictive and accurate equation of state (EOS). A rigorous classical treatment would combine a robust interatomic potential (including electronic and magnetic effects) for U of the solution as a function of V, an accurate configurational entropy of mixing (S_{mix}) expression accounting for structure, and the introduction of T via vibrational phonon frequency theory (Fultz, 2010). However, classical interatomic potentials need to be parameterized and cannot capture all subtle energetic effects; exact three-dimensional S_{mix} expressions are not available and must be approximated (e.g., the 1D chain of Ising (1925) or the coordination-number-dependent approximation of Pelton et al. (2000)); there is no fully predictive treatment of anharmonic effects for solids (Fultz, 2010) and our knowledge of atomic vibrations in liquids is limited (Bolmatov et al. 2012). In geochemistry, robust analytical treatments of condensed phases accounting for each contribution to the Helmholtz energy are generally not available. Instead one common empirical approach to P-V relations begins with analytical derivation of a compact interatomic potential (Vinet et al. 1987). However, most self-consistent approaches to date avoid an explicit interatomic potential via a quasi-harmonic finite strain free energy formalism (Davies, 1973). Such approaches depend on the quantity and quality of thermo-physical data for parameterization. In de Koker and Stixrude (2009), parameterization of such a model for single-component liquid phases using numerical experiments requires at least 16 adjustable parameters (for MgO) and at most 19 adjustable parameters (for SiO_2).

1.2 The challenge

In section 2 we will discuss the importance and limitations of experimental observations for parameterizing EOS models and will introduce the need for complementary constraints from numerical simulations. We will then discuss the level of accuracy that simulations must achieve in order to enable pure and multi-component phase equilibrium calculations. Chemical phase

Always consult and cite the final, published document. See http://www.minsocam.org or GeoscienceWorld

equilibria are sensitive to remarkably small energy differences, such that effects that may appear negligible in physical treatments of a single phase EOS become important. We will highlight the special challenges associated with simulating liquids and point out where the techniques commonly used in performing and interpreting ab initio molecular dynamics (AIMD) simulations, well-established in the study of solids, may not describe liquids well. In particular, the chemical complexity of silicate melts requires large numbers of atoms in the simulation and long run times. Ergodicity, a prerequisite for obtaining accurate transport properties, may take a long time to establish and, worse, apparently ergodic states with poorly equilibrated short range order may persist over even longer run times. It is difficult to establish criteria for complete sampling of the partition function except by (computationally expensive) approaches from multiple initial conditions with different degrees of internal order. Even though a simple test to judge the ergodicity of MD simulation data exists — plotting the logarithm of the mean square displacement as a function of the logarithm of time (Morgan and Spera 2001a, 2001b; Tikunoff and Spera 2014) — it is unclear how numerically sensitive internal energy and volume are to slightly non-ergodic conditions. As a result, the distinction between a deeply supercooled metastable liquid and a glass needs further exploration which goes beyond the scope of the present paper. We will close with a summary of recommendations for experimental, computational, and thermodynamic workers in this field.

2. Context and Motivation

2.1 The experimental approach

Ideally, all available experimental techniques would be used to provide sets of self-consistent thermo-physical data for the silicate melts and solids relevant to the Earth's interior. Experiments spanning adequate ranges of T, P and composition would optimally constrain the parameters of

Always consult and cite the final, published document. See http://www.minsocam.org or GeoscienceWorld

an EOS and mixing relationships for each potential stable phase. Then parameterized Helmholtz or Gibbs energy models for those phases would be considered in global constrained minimization algorithms such as MELTS (Ghiorso et al. 2002) or FACTSAGE (Bale et al. 2009) to predict complex phase equilibria in the Earth. Transport properties may also be fitted to experimental data using relatively simple forms such as Arrhenius or Adam-Gibbs laws.

Indeed, a great variety of experimental data on properties of natural and synthetic silicate melts, solids and glasses are available for this purpose. Chemical order and local chemical environment (a few nm) around cations or anions can be studied using nuclear magnetic resonance spectroscopy (Putnis, 1996), extended X-ray absorption fine structure (Simon et al. 2013) and X-ray diffraction (Sugiyama et al. 1996). Chemical diffusivity of many species has been measured, generally at intermediate scales (μm to mm); see compilations of Brady (2013), Zhang and Ni (2010); Zhang et al. (2010) or Lesher (2010). Density of silicate melts, solids and glasses is studied at macroscopic scale (mm to cm) by Archimedean methods (Lange and Carmichael, 1987), shock compression (Asimow and Ahrens, 2010), and X-ray absorption (Sakamaki et al. 2009, 2010a, 2010b, 2011). Viscosity is studied at macroscopic scale using devices such as rotational or parallel-plate viscometers (Del Gaudio and Behrens, 2009; Urbain et al. 1982) and creep apparatus (Neuville and Richet, 1991). Relaxation effects, i.e. the time-dependence of all of these properties, can be studied with techniques such as dilatometry, differential thermal analysis, calorimetry and viscometry (see Sipp and Richet (2002)). Chemical potentials or thermodynamic activities of species in silicate melts can be determined by electromotive force measurements (Sterten and Maeland, 1985), Knudsen effusion cell and mass spectrometry (Zaitsev et al. 2000), or via heterogeneous equilibrium between a melt and a mineral or a probe phase such as liquid (Rein and Chipman, 1965) or solid (Chamberlin et al. 1994) metallic alloy.

Always consult and cite the final, published document. See http://www.minsocam.org or GeoscienceWorld

Considering specifically the thermo-physical behavior of silicate melts at $P \geq 10$ GPa, however, fewer experiments are available. Shock compression of silicate melts, following Rigden et al. (1988), defines the *P*-*V*-energy EOS via the Rankine-Hugoniot equations. This technique has been extended to ~150 GPa and ~10000 K (Asimow and Ahrens, 2010) using gas guns and in a few cases to TPa pressures using laser compression (Hicks et al. 2006; McWilliams et al. 2012; Spaulding et al. 2012). The *P*-*T* paths of these experiments are governed by the physics of shock compression and manipulation of the initial condition or application of novel drive paths are needed for states hotter or colder than the principal Hugoniot. The extent to which this technique explores fully equilibrated states requires careful evaluation, although derived equations of state generally extrapolate consistently from known low-*P* values and the very high *T* of shock states suggests rapid relaxation (Rigden et al. 1988). Nevertheless, shock rise times are short (~10^{-10} s for liquids relevant to the earth's mantle) and this may be insufficient for complete relaxation of the chemical arrangement at the atomic level (called hereafter chemical short range order, SRO), particularly in highly multicomponent or topologically complex liquids. The extent to which all possible cation-cation second nearest neighbor (2NN) distributions are explored, and the equilibrium distribution located, can be estimated from the Einstein relation for diffusion and the self-diffusivity of Si. Experiments (Poe et al. 1997) and AIMD simulations (de Koker et al. 2008; Karki et al. 2007) show that this self-diffusivity strongly decreases as the degree of polymerization of the silicate melt increases. AIMD simulations also predict decreasing self-diffusivity with increased *P*. If the duration of shock compression and the resulting migration distances of Si cations do not allow enough permutations of the cation distribution, then chemical SRO cannot evolve; the chemical structure becomes frozen and does not reach the equilibrium state. As internal structure, quantified by the amplitude of the SRO, may evolve in

Always consult and cite the final, published document. See http://www.minsocam.org or GeoscienceWorld

non-ideal solutions as a function of composition, T and P, this suggests that shock compression measurements may not be able to capture the configurational entropy correctly.

Considering the ensemble of available data, then, empirical calibration of self-consistent thermodynamic properties of silicate phases is not yet possible at the level of accuracy to which one might aspire. Experimental limitations and cost lead to scarcity and inconsistency in thermo-physical data for silicate melts, solids and glasses, specifically at high T and P. Missing, imprecise or inaccurate experimental data in turn limit our ability to constrain the parameters of complex functional forms for the EOS over the entire range of relevant compositions. We must turn to simplified mixing rules to interpolate among studied compositions of liquid, solid and glass solutions. Various mixing rules for different thermo-physical properties of solutions at constant P and T have been proposed in the literature. It is common practice in geochemistry (de Koker et al. 2013; de Koker and Stixrude, 2009; Ghiorso et al. 2002) to model the energetic behavior of silicate solutions assuming that the S_{mix} in these multicomponent systems is ideal according to some selected definition. Excess heat capacity and excess molar volume of liquid solutions upon mixing are commonly taken to be zero and, in general, linear interpolation of the molar heat capacity and volume between available chemical compositions appears to describe the behavior of silicate liquids (Ghiorso et al. 2002; Lange and Carmichael, 1987). This leaves the enthalpy of mixing (H_{mix}) as the sole excess property to capture the non-ideal solution properties of such liquids. Laboratory data itself can have systematic and composition-dependent errors, so this general thermodynamic approach may become rather inexact unless coupled to constraints from numerical experiments. When many excess parameters (both enthalpy and entropy parameters) are required to accurately fit the set of available thermodynamic data (see for example the work of de Koker et al. (2013) on the MgO-SiO_2 system), it is unclear whether

Always consult and cite the final, published document. See http://www.minsocam.org or GeoscienceWorld

this reflects internal inconsistency in the calibration data, poor choice of functional forms for interpolation, or true complexity of the studied solutions.

2.2 The computational approach

Given gaps and shortcomings in experimental data, a promising way to refine and parameterize theories of phase properties is through numerical experiments, i.e. simulations of the individual and collective behavior of atoms via molecular dynamics or Monte Carlo methods. In these simulations, U of a given structure can be evaluated using classical interatomic potentials or quantum physics via density functional theory (DFT). Classical potentials contain empirical parameters and therefore hardly represent a replacement for experiments; on the other hand, DFT calculations are often referred to as ab initio techniques since in principle they do not depend on experimental input. In practice, the adjustment of some parameters is needed to represent the physical behavior of condensed structures. The cutoff energy, valence state, and cutoff radii for the partial waves are needed when building pseudo-potentials as well as in the projector augmented-wave (PAW) method to mimic all-electron wave functions (Kresse and Joubert, 1999). The convergence test or parameterization methodology used to adjust these parameters is typically not fully objective (see the methodology of Garrity et al. (2014) and of Jollet et al. (2014)).

Technically, such convergence tests should be conducted for each studied structure, as the convergence behavior appears to be structurally/chemically dependent according to benchmark testing of pseudo-potentials applied to several unary and binary compounds of different crystallographic structures by Garrity et al. (2014). The evident popularity of DFT in the scientific literature as a numerical tool to understand and explore the thermo-physical behavior of condensed phases relies on an optimum tradeoff between accuracy, transferability and

Always consult and cite the final, published document. See http://www.minsocam.org or GeoscienceWorld

computational efficiency, which has motivated compilation of optimal sets of these parameters. Examples of such libraries for several elements of the periodic table can be found, for example, in the recent work of Jollet et al. (2014) for the PAW method and in the work of Garrity et al. (2014) for the generation of pseudo-potentials. It is to be noted that there could exist cases where pseudo-potentials are used under conditions of strong compression (perhaps at terrestrial mantle pressures) that induce very short bond lengths. In this scenario, the transferability of the pseudo-potentials and the final precision of the resulting calculations could be severely impaired, which is not a topic frequently covered in the geochemical literature. As an example, the frozen core approximation typically used when building pseudo-potentials failed in the work of Pickard and Needs (2011) where they studied the behavior of solid lithium at pressures up to 2000 GPa. In this case, the 1S core electrons overlap on neighboring atoms under strong compression. For these reasons, very high quality pseudo-potentials in which all three electrons are treated explicitly are required in this case.

Moreover, the parameterization of a correlation energy function (Perdew and Wang, 1992) for charged bosons and fermions is required to account for the non-interacting electron-gas hypothesis of DFT; this is done, for example, by the quantum Monte Carlo method of Ceperley and Alder (1980).

Static calculations allowing the evaluation of the equilibrium V, the bulk modulus and its pressure derivative for various structures in their ground state are often used to determine the validity of DFT calculations through comparison with available experimental data. Wentzcovitch et al. (2010) presented an extensive literature review of DFT calculations applied to mantle minerals and highlighted the importance of correcting ground state calculations to account for thermal effects even with 300 K experimental data. Semi-classical lattice dynamic methods such

Always consult and cite the final, published document. See http://www.minsocam.org or GeoscienceWorld

as the quasi-harmonic approximation (Born and Huang, 1969) introduce the effect of atomic vibrations in the description of the Helmholtz energy, providing a useful and relatively robust method of estimating vibrational entropy and enthalpy for *P*-*T* ranges relevant to Earth's mantle (Wentzcovitch et al. 2010). For solids, the phonon dispersion needed to evaluate the vibrational excess energy is obtained from density-functional perturbation theory (Baroni et al. 2001).

The effect of *T* on thermo-physical properties can be accounted for more explicitly, up to and above the melting point, using Molecular Dynamics (MD). In this simulation scheme, Newton's equations of motion are solved iteratively to describe the paths of individual atoms in a structure (solid, liquid or glass) subject to periodic boundary conditions by determining the forces acting on them. The exploration of thermodynamic ensembles such as the isobaric-isothermal (NPT) ensemble and the canonical (NVT) ensemble requires the implementation of a thermostat, typically the Nosé-Hoover thermostat (Evans and Holian, 1985). Forces acting on atoms required in MD simulations can be described by either classical interatomic potentials or DFT.

The need for and promise of such numerical experiments is clear, and reviewing the entire literature of both classical and ab initio MD simulations relevant to Earth's mantle is beyond the scope of this work. However, conclusions of recent AIMD studies that "*they are now capable of treating chemically rich systems with multiple stable phases and extensive solution"* (de Koker et al. 2013) motivate the present discussion. As explained by Schubert et al. (2001), the earth's bulk composition is constrained, in part, by the cosmic material believed to be the primordial building blocks of the earth, e.g. the CI chondrites. It is generally accepted that the mantle is mostly peridotite and that the core is mostly iron as discussed in detail by McDonough and Sun (1995). The original pyrolite model of Ringwood (1962), refined by McDonough and Sun (1995), informs us that the earth's mantle is dominated by the SiO_2-MgO-"FeO"-Al_2O_3-CaO 5-major

Always consult and cite the final, published document. See http://www.minsocam.org or GeoscienceWorld

component system. However, the Cr_2O_3, Na_2O, TiO_2, MnO and other minor as well as volatile components may also drastically alter the thermo-chemical properties of the different mantle phases, the stability relations among those phases, and hence the geochemical evolution of the silicate Earth. Moreover, classical thermodynamics shows that phase equilibria are sensitive to small shifts in any of the free energy functions of the system. A difference of $\sim 10^2$ J/mol (1 meV/atom) in the thermodynamic description of a phase can shift a eutectic reaction by $\sim 10^2$ K or change the computed phase assemblage for imposed equilibrium conditions.

It is therefore important to explore whether such precision has been (or can be) achieved. We argue here that the chemically-rich terrestrial mantle silicate system and all its associated potentially stable phases cannot be studied accurately with the presently available numerical tools. The basis for this claim lies both in the theoretical and practical limits of standard DFT itself — including difficulty handling van der Waals type forces (Vuilleumier et al., 2009), hydrogen bonds (Dyer and Cummings, 2006), and compositions rich in transition metals such as Fe (requiring hybrid functionals to handle strongly correlated d-orbitals, e.g. Alfredsson et al., 2005) — as well as the theoretical and practical limits of molecular dynamic simulations based on DFT-derived forces. MD simulations endeavor to define the thermo-physical behavior of macroscopic, real solutions through the behavior of a limited number of atoms sampled for a limited period of time. It is of fundamental importance to analyze how picosecond (10^{-12} s) numerical experiments on hundreds of atoms ($\sim 10^{-22}$ mol) with periodic boundary conditions can be scaled up to represent the macroscopic behavior of condensed phases (moles) which can be observed evolving towards equilibrium on timescales of hours ($\sim 10^3$ s) to years ($\sim 10^7$ s).

Based on ideas from classical thermodynamics and results presented in the literature, this work examines the likely limitations of current state-of-the-art atomistic simulations of silicate melts.

Always consult and cite the final, published document. See http://www.minsocam.org or GeoscienceWorld

We believe that a critical review is needed at this time, with several goals in mind. We hope to motivate the reassessment of important systems using both classical MD and AIMD simulations, to identify key experimental investigations that can better constrain theories, to encourage progress in the definition and parameterization of interatomic potentials, to encourage authors to report more of their statistical analysis and resulting errors when performing MD simulations, and to suggest the need for hybrid strategies that build on the power of MD while overcoming computational limitations. We focus on three aspects of MD simulations that have received relatively limited scrutiny: 1) general kinetic limitations inherent to the classical treatment of atomic motions under periodic conditions; 2) the consequence of the extreme cooling/heating rates of MD simulations for potential phase transitions; and 3) the homogenization times sufficient for liquid structures, especially at low T or high P, to equilibrate the local chemical environments of the atoms, quantified by the amount of short range order.

3. Configurational entropy of mixing in the chemical sense

It is important at the outset to define some important concepts underlying the idea of chemical SRO. First, let us attempt to define the configurational entropy of mixing, i.e. the entropy (distinct from and in addition to vibrational entropy) arising from the availability of numerous distinct arrangements of atoms in a mixed solution phase. Figures 1a and 1b show the theoretical range of possible S_{mix} as a function of composition in the binary atomic systems Mg-O and Si-O. The reference basis is set by the total number of atoms needed to define the MgO (2 atom basis) and the SiO_2 (3 atom basis) pure oxides. At the stoichiometric compositions MgO and SiO_2, S_{mix} can be no smaller than 0 J mol^{-1} K^{-1} (inverted triangles) — which describes the limit of only one possible configuration of the atoms — and no larger than the ideal maximum (stars) S_{mix} corresponding to random permutation of all the atoms. The minimum is achieved for solid MgO-

Always consult and cite the final, published document. See http://www.minsocam.org or GeoscienceWorld

300 periclase and SiO_2-low quartz at 0 K, where the equilibrium concentration of all defects with
301 positive substitution energy goes to zero. The maximum S_{mix} for each oxide implies that the
302 internal structure of the solution is equivalent to that of an ideal gas; the atoms are not interacting
303 with each other and there is no correlation between atomic positions in the solution. Chemical
304 interactions between cations and anions in liquid MgO and SiO_2 must necessarily yield S_{mix} for
305 each system between these two limits.

306 In Figure 2, S_{mix} of the MgO-SiO_2 system is presented for two different reference states. In
307 Figure 2a, Mg, Si and O atoms define the reference state. The maximum configurational entropy
308 in this case is 20 J mol^{-1} K^{-1}, but this can only be equated to S_{mix} along the binary if the
309 configurational entropies of pure MgO and SiO_2 are both equal to 0. On the other hand, if fully
310 disordered MgO and SiO_2 are used as reference state (figure 2b), then a maximum of 6.05 J mol^{-1}
311 K^{-1} can be reached. Finally, if MgO and SiO_2 are treated as associates a configurational entropy
312 of mixing of 5.76 J mol^{-1} K^{-1} is obtained at the equimolar composition. This is the so-called
313 ideal S_{mix} relative to the oxide end members. In this case, MgO and SiO_2 entities are assumed to
314 be indistinguishable in the chemical sense. For silicate melts, first nearest neighbors are
315 exclusively strong cation-anion energetic interactions. Therefore, it is more reasonable to assume
316 that the amplitude of S_{mix} will be in the range of values obtained from the associate model.

317 These important notions regarding the limiting behavior of S_{mix} appear to have been neglected in
318 recent AIMD studies. A maximum S_{mix} of about 18 J mol^{-1} K^{-1}, proposed by de Koker et al.
319 (2013) using their coordination state model (de Koker and Stixrude, 2009) requires both that the
320 configurational entropies of pure MgO and SiO_2 liquid relative to the atoms are close to zero and
321 that the mixing of these two liquid oxides results in a completely randomized solution (S_{mix} of an
322 ideal gas), which seems unreasonable. While cations in different coordination states yield more

Always consult and cite the final, published document. See http://www.minsocam.org or GeoscienceWorld

possible configurations than fixed coordination numbers, the resulting number of configurations surely should not approach that of totally random and uncorrelated atomic positions. It should be emphasized here that AIMD simulations do not provide direct access to the entropy of the studied structure. As explained by de Koker et al. (2013), S_{mix} of the liquid phase in the MgO-SiO_2 system must be parameterized by fitting experimental observations such as the 1 atm liquidus temperatures for periclase and forsterite together with the immiscible liquid field.

Another clear indication that the general concept of S_{mix} and its limiting behavior are not consistently applied in the MD simulation literature is provided by Karki et al. (2013), where configurational entropy is evaluated using the Adam-Gibbs theory (Adam and Gibbs, 1965) to represent the T-dependence of the melt viscosity obtained from the same AIMD simulations. The Adam-Gibbs theory gives a maximum S_{mix} of 2.5 J mol^{-1} K^{-1} close to X_{SiO_2} = 0.4 (Karki et al. 2013) (Figure 3). The amplitude of the maximum S_{mix} inferred from viscosity is more than 7 times less than that inferred from the coordination state model applied to the same simulations. This discrepancy could be an issue with the simulations themselves (the results for viscosity at different T might not be comparable and might lead to anomalous fits to Adam-Gibbs theory) or it might be an issue with the thermodynamic model and its definition of configurational entropy. Obviously, the underlying assumptions leading to the Adam-Gibbs theory, i.e. that the relaxation time is a function of the macroscopic configurational entropy and that the viscosity follows an Arrhenius-like behavior, must be valid in order to estimate this thermodynamic property from viscosity data alone, as discussed by Dyre et al. (2009).

These observations suggest a need to test the precision of the AIMD simulation results and the resulting thermodynamic model of de Koker et al. (2013) to see whether it accurately predicts experimental measurements for this system not considered in the parameterization process,

Always consult and cite the final, published document. See http://www.minsocam.org or GeoscienceWorld

especially in the SiO_2-rich region. Available data include the SiO_2 activity in silicate melts at 1 atm (Kambayashi and Kato, 1983, 1984); the evolution of the consolute point of the miscibility gap in the silica-rich region as a function of *P*, indirectly measured by Hudon et al. (2004, 2005); and the liquidus surface for crystallization of coesite in this system at 5 GPa, measured by Dalton and Presnall (1997).

4. General considerations about kinetic limitations of MD simulations

4.1 *Immiscibility*

The most recent AIMD study of the MgO-SiO_2 system by de Koker et al. (2013) serves to introduce some technical issues in exploring the partition function of a multicomponent solution by MD simulation. First, note that equilibrium miscibility gaps are determined solely by the excess properties of the considered solution. Figure 4 shows raw enthalpy of mixing (H_{mix}) data from AIMD simulations of de Koker et al. (2013) at 2000 K and 0 GPa for different silicate melts. The "s" shape of the enthalpy of mixing (which is also obtained at 3000 K) is typical for a solution that tends to form immiscible liquids. Combined with the total entropy of mixing expression in the de Koker et al. (2013) thermodynamic model, this enthalpy of mixing induces a small miscibility gap in the range $0.8 \leq X_{SiO_2} \leq 1.0$ (Figure S15 of their work). Comparison of the predicted miscibility gap and experimental results of Hageman and Oonk (1986) and Ol'shanskii (1951) shows that AIMD simulations and thermodynamic model of de Koker et al. (2013) greatly underestimate the width of the solvus, although the consolute *T* at 1 atm is close to that of Hageman and Oonk (1986). Nevertheless, both the experimental and predicted miscibility gaps show that $MgSi_5O_{11}$, one of the simulated compositions, should be inside the two-liquid region. Simulation of this composition, however, yields a single liquid phase with a positive enthalpy of

Always consult and cite the final, published document. See http://www.minsocam.org or GeoscienceWorld

mixing even though the equilibrium state should be a two-liquid assemblage. This is of concern, whether or not this composition lies inside the spinodal region: if inside the spinodal region, the $MgSi_5O_{11}$ melt should spontaneously decompose into silica-rich and MgO-rich liquids, which clearly did not occur. If outside the spinodal region, the $MgSi_5O_{11}$ melt is metastable and should have been studied using an initial configuration that accounts for the immiscible behavior. In either case, the AIMD simulations do not reflect the true equilibrium state of this melt.

This is a clear example showing that AIMD simulations, applied to silicate liquids using short simulation times (3-6 ps) and ~100 atoms per studied supercell, may not explore the entire partition function. There are several examples in the literature that show that MD simulations are neither designed nor capable of ensuring complete sampling of partition functions, even after long simulation runs originating from a given initial configuration. The work of Schön et al. (2006) on ab initio computation of low-*T* phase diagrams exhibiting miscibility gaps show that, at elevated *T*, the locally ergodic regions of phase space are not necessarily localized around a single local minimum (Helmholtz energy surface), but may contain many such local minima. Likewise, Zhang (2011), performing AIMD simulations of MgO-SiO_2 liquids, found a standard deviation in enthalpy among runs using different initial configurations fully as large as the amplitude of the excess enthalpy of solution reported by de Koker et al. (2013). This does not imply that the simulations are non-ergodic; on the contrary it emphasizes the highly probable existence of several locally-ergodic minima that have to be explored in order to define the equilibrium state of the system correctly.

4.2 *Evolution of Short Range Order (SRO)*

Obtaining, in a simulation, a reasonable sampling of equilibrium configurations with the correct structural and physical properties requires the achievement of the correct degree of short-range

Always consult and cite the final, published document. See http://www.minsocam.org or GeoscienceWorld

order. We suggest that important insights concerning the procedures generally used in MD simulations of liquids and the extent to which they explore the SRO energy landscape can be found by examining well-documented studies of analogous phenomena surrounding a well-known solid-solid order-disorder phase transition in a simple binary system. From an internal chemical structure perspective, an order-disorder phase transition is highly relevant to our discussion of liquids, since it is driven by the vanishing of short-range chemical order; that a solid has long-range chemical order and a liquid does not is unimportant for this discussion. In particular, let us consider the example of the Au-Cu system, where the equimolar composition undergoes a first-order phase transition from a face-centered cubic (FCC)-$L1_0$ ordered structure to a FCC-disordered solution at a critical temperature $T_{O\rightarrow D}$ of ~ 685K (Cao et al. 2007), which is about $0.58T_{liquidus}$ at this composition. Similar order/disorder phase transitions also occur for the Cu_3Au and the $CuAu_3$ FCC-$L1_2$ ordered structures in this system.

All thermodynamic models that allow the representation of such a phase transition — e.g., the cluster variation method (Kikuchi, 1951) or the cluster site approximation (Oates and Wenzl, 1996; Oates et al. 1999) — predict the presence of some residual SRO above the phase transition. This SRO decreases to some extent with further increase of *T* beyond the transition point, whereas SRO in the disordered phase is expected to increase with increasing *P* for this system, at least in the low compression regime. As pointed out by Franzblau and Gordon (1967), the initial slope of the evolution of $T_{O\rightarrow D}$ as a function of *P* is defined by the Clapeyron equation: $\frac{\partial T_{O\rightarrow D}}{\partial P}=\frac{T_{O\rightarrow D}\Delta V_{O\rightarrow D}}{\Delta H_{O\rightarrow D}}$. A thermodynamic literature review of the Au-Cu system (Okamoto *et al*, 1987) then predicts that $\frac{\partial T_{O\rightarrow D}}{\partial P}>0$ at 1 atm; indeed $T_{O\rightarrow D}$ increases by ~10 % from 1 atm to 2 GPa for Cu_3Au (Franzblau and Gordon,1967). Under strong compression, the

Always consult and cite the final, published document. See http://www.minsocam.org or GeoscienceWorld

Clapeyron relation cannot be applied easily because $\Delta V_{O\to D}$ and $\Delta H_{O\to D}$ at elevated P are not available in the literature. Franzblau and Gordon (1967) also argue that the energy barrier (kinetic limitations) to disorder the Cu_3Au structure in this case should increase with P.

When starting from a perfectly ordered structure, MD simulations of FCC AuCu on a periodic lattice do not allow identification of the transition temperature even for the slowest heating rates. Experimentally, the order/disorder transitions in the Au-Cu system probably nucleate by macroscopic heterogeneous mechanisms such as surface segregations or antiphase boundaries, as discussed by Hayoun et al. (1998) in Cu_3Au. Numerically, however, the atomic permutations needed to modify the chemical order and induce this order/disorder transition face major kinetic limitations: to permute two nearest neighbor atoms in a periodic defect-free lattice requires an energetically unfavorable Frenkel defect (substitutional vacancy + interstitial atom). When T increases, the structure generally expands, reducing the energy cost of a Frenkel defect. As the energetic cost of a Frenkel defect approaches k_BT, atoms start to permute, but this is typically far above the observed critical T of solid-solid order-disorder transitions. As defects accumulate in this T range, the solid structure loses mechanical stability and undergoes mechanical fusion. For FCC gold, e.g., mechanical fusion occurs in MD simulations using the interatomic potential parameterized by Lee et al. (2003) at around $1.3T_{liquidus}$ (compare to $T_{O\to D} \approx 0.58T_{liquidus}$ in AuCu). This implies that MD simulations can explore a superheated FCC structure up to this T.

Above the mechanical fusion temperature, liquid state MD simulations of metallic systems should not be too sensitive to the initial configuration because permutations of first nearest neighbor pair fractions that define the chemical order are energetically inexpensive, even when performed in a random motion fashion. For the same reason, it is a common practice to use high T and large volume to melt initial solid structures in MD simulations. However, applying high P

Always consult and cite the final, published document. See http://www.minsocam.org or GeoscienceWorld

436 to mechanically melted structures should be done with care: imposing high *P* increases the
437 energetic cost of modifying short-range chemical order, as discussed above. In this case, MD
438 simulations might not be able to explore enough chemical configurations to populate the
439 partition function adequately. Monte Carlo simulations (Metropolis et al. 1953) are therefore
440 preferred when thermodynamic properties based on statistical analysis are to be obtained for
441 solid and liquid structures, as the technique allows one to span the partition function much more
442 efficiently.

443 The analogy of the energetic barrier kinetic limitation to disordering of solid structures extends
444 to silicate melts as follows. It is evident that silicate melts are defect-rich, low-symmetry
445 structures less prone to this problem. However, when *P* increases or *T* decreases, there is no
446 general rule to predict how the kinetic energy barrier between two states of internal energy
447 compares to k_BT (even if the equilibrium *U* difference between the states is small), especially
448 considering the fact that the atoms follow a random walk inside the simulation box (Brownian
449 motion). In other words, atoms are not specifically seeking minimum energy transition states.
450 This is an important issue that was raised in early MD simulations works (see for example Alder,
451 1964). For this reason, it is of fundamental importance to start several MD simulations with
452 initial configurations differing in their SRO to test how the initial structure affects the derived
453 thermo-physical properties. To our knowledge, such a systematic study for silicate melts under
454 pressure has not been published in the literature yet. However, the provocative MD study of
455 MgO-SiO_2 melts by Zhang (2011) justifies further work; they examine three distinct initial
456 configurations for each composition and obtain average properties with standard deviations from
457 10 to 50 kJ/mol. Even though the total simulation time might have been too small for silica-rich
458 melts to adequately relax their structures (only 6 ps), it appears evident from this study that the

Always consult and cite the final, published document. See http://www.minsocam.org or GeoscienceWorld

uncertainty due to initial configuration in the evaluation of a mixing property could be of the same order of magnitude or even larger than the property itself.

4.3 *Self-diffusivity*

Another kinetic limitation inherent to the chemical nature of MD simulated silicate melts is the limited self-diffusivity of the various species. In the NVT or NPT ensembles that are typically explored in earth science studies, the homogenization or evolution toward the equilibrium state of simulated melts is ensured solely by self-diffusion of the atoms (the system is not sensitive to chemical potentials in these ensembles). If the total MD simulation time at a given applied P and T is too short compared to self-diffusion time-scales, then the system will not have enough time to reach the equilibrium state. The severity of this kinetic limitation in the approach to equilibrium for high P (or low T) silicate melts can be characterized using self-diffusivities from the MD simulations themselves. Ghosh and Karki (2011) presented AIMD simulations of Mg_2SiO_4 melt at high P in order to evaluate self-diffusivity and viscosity. These authors noted two simulations, at compressed volumes of $0.6V_X$ (3000 K and 67 GPa; V_X is the volume at 3000 K and 0 GPa) and $0.5V_X$ (4000 K and 159 GPa) that displayed glass-like rather than liquid-like dynamics, in which mean square displacements remained below 10 $Å^2$ for all species even for runs of 300 ps. This observation makes perfect sense from a self-diffusivity perspective. The self-diffusivity of Si is about 5 x 10^{-11} m^2/s under these conditions (Ghosh and Karki, 2011). To permute two Si-Si second nearest neighbor cations (distance of 3 Å according to Karki et al., 2007), a time of about 300 ps is required:

$$\left(6 \cdot D_{Si-Si} \cdot t\right)^{1/2} = \left(6 \cdot 5x10^{-11} \frac{m^2}{s} \cdot 300\,x10^{-12} s\right)^{1/2} = 3Å \qquad (1)$$

Always consult and cite the final, published document. See http://www.minsocam.org or GeoscienceWorld

Indeed, 300 ps is the maximum simulation time the authors used. Under these simulation conditions, the SRO defined by 2NN pairs remains almost constant. Similar kinetic limitation examples can be found in the work of Karki et al. (2007) and Lacks et al. (2007) for liquid SiO_2. In these studies, equilibrium conditions inducing kinetic limitations can be identified by looking at the slope of log-log plots of the mean square displacement as a function of time, which should be equal to one in the diffusive regime. The systematic application of such a "kinetic" test to identify the state (i.e. liquid or glassy) of the supercell in MD simulations can be found, for example, in the work of Morgan and Spera (2001a, 2001b). In general, however, MD simulations do not present such evaluations of the kinetic relaxation, even when computing transport properties.

Another clear example showing the importance of self-diffusivity on homogenization and relaxation of simulated structures in MD can be observed for liquid MgO. In MgO melts, the self-diffusivity of Mg is ~8 x 10^{-9} m^2/s at 3000 K and 0 GPa according to Karki et al. (2006) (a factor of 160 higher than Si in liquid SiO_2 at 3000 K). There is a clear agreement (Karki et al. 2006, 2013; Lacks et al. 2007) that MD simulations of 2-5 ps are sufficient to generate accurate results ($d_{Mg\text{-}Mg} \approx 3$ Å), which is consistent with the application of Equation 1. Similarly, Martin et al. (2012) set a self-diffusion cut-off of 10^{-9} m^2/s in their study of the 1-bar eutectic melt in the system $CaAl_2Si_2O_8$-$CaMgSi_2O_6$ in order to ensure ergodicity, which induces a mean travel distance for oxygen of 3.2 Å (twice the anion-cation separation) in 50 ps, which appears to be equivalent to the present criterion.

The kinetic limitations to achievement of equilibrium SRO presented in this section could be the main cause of the apparently non-equilibrium results presented in Figures 3 and 4.

4.4 Effect of the cooling rate in MD simulations on the resulting studied structure

Always consult and cite the final, published document. See http://www.minsocam.org or GeoscienceWorld

Silica glasses were studied by Vollmayr et al. (1996) using MD simulations. The authors mentioned that the studied cooling rates were between 1.14×10^{15} and 4.44×10^{12} K/s, which are many orders of magnitude larger than laboratory rates. In the work of de Koker et al. (2008) on Mg_2SiO_4 liquid, the "slow cooling rate" of their AIMD simulations is 1.0×10^{15} K/s (3000 K in 3000 fs), which is again about 10 orders of magnitude higher than typical cooling rates used to produce silicate glasses. As an example, Revcolevschi (1976) estimated the cooling rate of an eutectic NiO-CaO liquid in a splat quenching apparatus to be 2.6×10^{5} K/s.

According to the equation parameterized by Vollmayr *et al.* (1996) for the glass transition temperature of silica, the cooling rate of de Koker et al. (2008) would induce a glass transition for pure silica above 4000 K at atmospheric pressure. Furthermore, increasing pressure for a given cooling rate will increase the glass transition temperature (see Martin et al. 2012). This glass transition temperature for silica is higher than any observable glass transition temperature (higher even than the liquidus temperature) but the important point is that structural relaxation may not continue below 4000 K or higher in these simulations, and the state of order recorded at lower temperature seems unlikely to represent equilibrium.

5. Large-scale classical MD simulations vs. small-scale AIMD simulations

Classical MD simulations exploit the fast evaluation of forces to achieve much longer simulation times and numbers of simulated atoms. Each of these advantages contributes to the higher precision of classical MD in distinct ways. Concerning the number of atoms, Ghiorso and Spera (2010) presented all the advantages of using large scale simulations to access the most accurate thermo-physical properties of silicate melts. It is clear that large MD simulations allow better statistics: sampling over more atoms yields more countable first nearest neighbors, second nearest neighbors, etc. For a closed packed FCC-like structure, with 70 atoms (typical of AIMD

Always consult and cite the final, published document. See http://www.minsocam.org or GeoscienceWorld

simulations), there would be 420 distinct 1NN pairs to analyze; for a system of 10^4 atoms (typical of classical MD), there would be 6 x 10^4 1NN pairs. Furthermore, number of atoms contributes to uncertainty in evaluating both T (induced by the thermostat) and P: McQuarrie (2000) reported that this uncertainty scales as $N^{1/2}$. Finite-size effects caused by a small number of atoms are often argued to be insignificant in AIMD studies (de Koker and Stixrude, 2009; Karki et al. 2006, 2007), although the evidence supporting this claim is generally difficult to evaluate quantitatively. On the contrary, several classical MD simulations quantified this effect (Horbach et al. 1996; Saksaengwijit and Heuer, 2007; Yeh and Hummer, 2004; Zhang et al. 2004). The general consensus of these studies is that, while thermodynamic properties appear to be insensitive to system size, dynamic properties such as self-diffusivity and viscosity can be quite sensitive. However, studies that suggest limited system size is adequate for assessing thermodynamic properties are all applied to pure chemical systems. In multicomponent systems, the number of different types of 2NN pairs to explore and the swap distances needed to exchange different cations are much larger. The system size effects in multicomponent systems have not been comprehensively evaluated, either with regard to major components or dilute components.

Reaching the equilibrium state in a pseudo-unary system is fast (no kinetic limitations related to self-diffusivity), even when the high symmetry of a solid structure has to be broken in order to reach equilibrium. The classical solid-liquid interface MD simulation study of Soules et al. (2011) demonstrates this principle, showing that the phase boundary interface propagates much faster than atomic displacements caused by self-diffusivity. For pseudo-unary systems such as liquid SiO_2, dominated by indistinguishable tetrahedral entities, distinct chemical species make little contribution to configurational entropy. The situation might be slightly different when pressure is increased, as different entities become significant in the melt. As reported by Karki et

Always consult and cite the final, published document. See http://www.minsocam.org or GeoscienceWorld

549 al. (2007), the Si-O coordination number shifts from 4 at ambient pressure to 6.5 at 150 GPa.
550 Therefore, there might be equilibrium conditions for which distinctions between different stable
551 entities have to be accounted for in the description of the configurational entropy of the solution.
552 However, conversion among differently coordinated cations requires only small displacements of
553 the oxygen anions and so coexistence of different coordination states probably does not imply a
554 substantial increase in necessary simulation time. Hence, relatively short simulation times should
555 allow exploration of the partition function for such unary/pseudo-unary systems. To evaluate
556 dynamic properties, the shortest simulation time should allow at least one "equivalent" cation-
557 cation permutation. For liquid silica, all authors in the literature (for both classical MD and
558 AIMD studies) (Karki et al. 2007, 2013; Lacks et al. 2007) appear to agree that a simulation of
559 0.3-1 ns is required to evaluate the viscosity and self-diffusivity (5×10^{-11} m^2/s at 3000 K and 0
560 GPa) in liquid silica, which is about the minimum time to allow one Si-Si cation-cation
561 permutation (~3Å) (see equation 1).

562 For MD simulations of multicomponent systems, the situation is quite different. A sampling of
563 2NN pair fractions sufficient to obtain the average equilibrium proportions, given the long
564 distances between cations that arise (ex.: $d_{Si\text{-}Si}$, $d_{Mg\text{-}Mg}$, $d_{Mg\text{-}Si} > 3$ Å according to Zhang (2011) for
565 $MgSiO_3$ melt at 0 GPa and 4000 K), should require a simulation of at least several ns, especially
566 for silica-rich melts (based on self-diffusivity of Si in liquid SiO_2 at 3000 K). In this case, the
567 thermo-physical data required to parameterize a silicate melt EOS would be accurately obtained,
568 as several cation-cation permutations would occur in the course of the simulation.

569 For shorter simulations, the accuracy depends on the energetic differences among configurations.
570 If chemical ordering is a minor contribution to *U*, the average internal energy from MD

Always consult and cite the final, published document. See http://www.minsocam.org or GeoscienceWorld

simulations may accurately describe the true equilibrium U of the system. Also in this case, the assumption of ideal S_{mix} (suitably defined) would be fully consistent with the MD simulations and the resulting Gibbs (or Helmholtz) energy would also be accurate.

In contrast, if chemical ordering significantly affects U, then it is unclear if MD simulations of several ns are sufficient to accurately parameterize an EOS of silicate melts. Imagine a system where short range order is important enough to result in S_{mix} appreciably lower than the ideal value. Energy differences between distinct configurations could be large. Energy fluctuations during a single MD simulation run with thousands of atoms traveling for several ns might not capture this particularity of the system. The average U obtained from this MD simulation might still approximate thermodynamic U (if the initial configuration reflects on average the equilibrium chemical ordering of the system) but properties related to fluctuations (instantaneous heat capacity, instantaneous thermal expansion, Grüneisen parameter, etc) would not be captured well. This is one reason why 2^{nd}-order derivative parameters are generally better estimated from thermodynamic models fitted to many simulation points, rather than directly extracted from time-dependent simulations. In this context, starting with different initial solid structures (all ordered in some way, by definition) and subsequently melting them at high T to see if the liquid retains memory of the initial state (see Stixrude and Karki (2005) and de Koker et al. (2008)) will not diagnose these issues. This is a different test from starting with different liquid configurations with distinct chemical ordering to see if MD simulations present similar statistics, as proposed by Zhang (2011).

Finally, in intervals of phase space where small T or P changes induce large increases in equilibrium chemical ordering, significant extra time may be needed to reach equilibrium after

Always consult and cite the final, published document. See http://www.minsocam.org or GeoscienceWorld

perturbation of *T*, *V* or *P*. In this case, running MD simulations of silicate melts even of several ns (typical for classical MD) might not be sufficient. Consider an MD simulation performed close to a consolute point (whose critical *T* is not known *a priori*). Cooling (or quenching, in MD simulations) a disordered liquid structure across an equilibrium exsolution boundary would reveal the miscibility gap only for simulation times long enough to allow species to segregate. To homogenize a simulation box for these conditions (relevant phase transitions generally occur at low *T* / high *P*) only by self-diffusivity and a random walk of atoms, long simulation times will be needed. With kinetic limitations (e.g., small free volumes available at elevated *P*), it may not ever be reasonable to use MD simulations alone to explore the partition function in this case. Monte Carlo simulations should be better able to study phase transitions driven by evaluation of chemical order (e.g. miscibility gaps, fragile-to-ductile liquid transition, order-disorder transition in solids, etc.).

6. Cautions concerning LDA pressure corrections in multicomponent liquid systems

It is well known that neither of the common exchange-correlation functionals used in DFT, the local density approximation (LDA) and the generalized gradient approximation (GGA), yields precise matches to the volume and compressibility of all phases (Karki et al. 2001). There are, however, well-established corrections, for example an empirical pressure correction to account for the under-estimation of molar volume due to overbinding in LDA (van de Walle and Ceder, 1999). Here we consider the magnitude of these corrections applied to multicomponent liquid systems and question whether uncertainty in such corrections is large enough to prevent useful definition of energetic mixing relations in materials of the Earth's mantle.

There is actually no physical theory specifying that LDA systematically induces overbinding or consequently underestimates equilibrium molar volume. Rather such a trend often arises in

Always consult and cite the final, published document. See http://www.minsocam.org or GeoscienceWorld

616 comparisons between ab initio calculations and experimental data. Thus there is no fundamental
617 understanding of how the error varies with composition or structure. Furthermore, in
618 consideration of oxide solids, Wentzcovitch et al. (2010) argued that the error is simply a matter
619 of applying static (0 K) LDA calculations to 300 K conditions. Combining quasi-harmonic
620 theory for vibrational effects with static DFT calculations (0 K) yields an almost perfect match to
621 experimental 300 K volumes of the solids examined in that study. In this scenario, the correction
622 to the static energetic stability of a structure, $\Delta U_{LDA\rightarrow \exp.}$,

623 $$\Delta U_{LDA\rightarrow \exp.} = \int_0^{S^{vib.}} TdS - \int_{V_0}^{V_{\exp.}} PdV \qquad (2)$$

624 arises from vibrational entropy effects alone; no mechanical work contribution (second term in
625 Equation 2) is needed. Likewise, AIMD simulations performed by Karki et al. (2006) for MgO
626 and by Karki et al. (2007) for SiO_2 using LDA, incorporating entropy effects via molecular
627 dynamics rather than quasi-harmonic theory, appear not to suffer from overbinding.

628 On the other hand, the same authors in more recent studies (de Koker et al. 2008, 2013; de Koker
629 and Stixrude, 2009) present a different and incompatible observation regarding the precision of
630 LDA-MD calculation of silicate melts, whose differences from experiment are once again
631 attributed to LDA overbinding. In this treatment, the mechanical work term in Equation (2)
632 rather than the vibrational entropy contribution to static LDA simulations is taken as the source
633 of LDA errors. Thus, in MD simulations where vibrational entropy effects are folded into the
634 internal energy contribution (*T* is mimicked by a thermostat), a systematic *P*-shift is applied to
635 the *P*-*V* EOS to account for overbinding effects (de Koker et al. 2008, 2013; de Koker and
636 Stixrude, 2009). This *P*-shift is calibrated as a function of composition only for those

Always consult and cite the final, published document. See http://www.minsocam.org or GeoscienceWorld

637 compositions where experimental solid volumes at 1 atm can be compared to NVT-MD
638 simulations at the same volume. This *P*-shift function is taken to be independent of structure and
639 applied to both solids and liquids of equal chemical composition. Moreover, the *P*-shift is
640 assumed to be adiabatic (no entropy contribution) and independent of the elastic moduli of the
641 material. The energy correction ΔU_{emp} simply becomes (de Koker and Stixrude, 2009):

642 $$\Delta U_{emp} = -P_{emp}\left(V - V_0\right) \quad (3)$$

643 Applying such a systematic correction to MD simulations is of uncertain validity and can have a
644 large effect on derived properties such as enthalpy of mixing. First, it is unclear that LDA does
645 systematically underestimate volume for geologically relevant systems when the zero-point
646 anharmonic expansion is considered, especially for ionic solids or condensed phases with partly
647 ionic chemical interactions, according to the study of Wentzcovitch et al. (2010). On the other
648 hand, it appears evident from the calculations performed by Haas et al. (2009) on 60 cubic
649 structures that LDA considerably underestimates molar volumes of solids at 0 K when compared
650 to available experimental data. Second, if the degree of overbinding depends on the nature of
651 chemical bonding in a material, then the changes in bonding character in silicate melts with *P* (de
652 Koker et al. 2008, 2013) renders it highly improbable that a constant *P* correction term based on
653 a 1 atm solid structure would be sufficient to account for the gradual shift toward differently
654 coordinated and more metallic-like chemical interactions in increasingly compact liquids.

655 Finally, the application of the *P*-shift scheme to multicomponent systems may introduce serious
656 errors. In their work, de Koker et al. (2013) estimated the *P*-shift as follows. Four anchor points
657 — solids of known volume at 1 atm — are available (MgO, Mg_2SiO_4, $MgSiO_3$, and SiO_2). Of
658 these, only SiO_2 is on the silica-rich side of the join. A quadratic polynomial fit to the four points

Always consult and cite the final, published document. See http://www.minsocam.org or GeoscienceWorld

659 was assumed by de Koker et al. (2013) (Figure 5). This is reasonable, but a *P*-shift that increases
660 linearly from MgO up to $MgSi_5O_{11}$ (open circle in Figure 5) and then sharply decreases towards
661 SiO_2 is equally plausible. This would lead to a "V-shape" *P*-shift, which resembles the V-shaped
662 curves for several important mixing properties in de Koker et al. (2013).

663 Table 1 presents an estimate of volumes at 0 GPa, V_0^{FST}, using the finite-strain EOS of de Koker
664 et al. (2013) for each MgO-SiO_2 melt composition, with the pressure correction term P_{emp} applied
665 by these authors removed. That is, the V_0 values in de Koker et al. (2013) are volumes at *P*
666 empirically corrected to 0 GPa, whereas here we fit instead the actual 0 GPa MD simulation
667 results. A short FORTRAN algorithm and parameter files are provided in the supplement to
668 implement the EOS of de Koker et al. (2013).

669 This exercise allows us to estimate the corrections to both internal energy, ΔU_{emp}, and enthalpy,
670 ΔH_{emp}, that should be applied for any functional form of the *P*-shift. Table 1 shows these results
671 for all compositions studied by de Koker et al. (2013) using the quadratic composition
672 dependence of P_{emp} and (in italics) results for $MgSi_5O_{11}$ liquid using the V-shaped *P*-shift from
673 Figure 5. This particular composition demonstrates the potential effect of the *P*-shift uncertainty
674 on the resulting thermo-physical properties because 1) it lies inside the miscibility gap at low *T*
675 and 2) its *P*-shift must be predicted from a certain arbitrary functional form.

676 Figure 6 shows how such a systematic correction induces a non-negligible excess enthalpy
677 correction $h^{xs}_{correction}$ defined as follows:

678 $$h^{xs}_{correction} = \left(\Delta H_{emp}\right)_{X_{SiO_2}} - \left[X_{SiO_2}\Delta H^{SiO_2}_{emp} + \left(1 - X_{SiO_2}\right)\Delta H^{MgO}_{emp}\right] \quad (4)$$

Always consult and cite the final, published document. See http://www.minsocam.org or GeoscienceWorld

679 with a shape mirroring the shape of the *P*-shift function. A series of MD simulations whose raw
680 enthalpy values suggest a substantial negative enthalpy of mixing (-8 kJ/mol) could be
681 transformed into a positive enthalpy of mixing entirely through the application of the *P*-shift. In
682 multicomponent melts, this could potentially invert the tendency to favor heterogeneous 2NN
683 pairs, favoring Mg-Mg and Si-Si pairs. The internal structure and S_{mix} should be modified in turn,
684 which is not accounted for in this simple correction scheme. Thus, while a small and constant
685 energetic LDA overbinding correction might be helpful in unary systems, extension of this
686 principle to multicomponent systems and to phases with different chemical bonding character is
687 unsupported. Moreover, differences among functions that might define the composition
688 dependence introduce differences in enthalpy corrections as large as the enthalpy of mixing
689 itself. Such uncertainties might lead to excess properties that are not accurate enough to predict
690 phase equilibria.

691 Besides the uncertain composition dependence of the LDA correction, there is direct evidence
692 that it also depends on the structure of silicate phases and therefore on the volume applied to
693 liquid silicates. Hamann (1996) showed that LDA-based DFT predicts that stishovite is slightly
694 more stable than quartz ($\Delta U_{Quartz \rightarrow Stishovite} = -0.05eV$) in the ground state at 0 GPa. Experimental
695 calorimetry by Holm et al. (1967) and Akaogi and Navrotsky (1984), however, show that quartz
696 is the more stable phase ($\Delta U_{Quartz \rightarrow Stishovite} \approx +0.52eV$). The most likely explanation is that the
697 error in LDA is not invariant to coordination number change and the energetics of the 4-fold
698 (quartz) to 6-fold (stishovite) transition do not benefit from the same error cancellation as EOS
699 curves applied to a fixed crystal structure.

700 There are other concerns with the use of LDA for multicomponent mantle materials. An
701 electronic entropy contribution to the Helmholtz or Gibbs energy may need to be considered at

Always consult and cite the final, published document. See http://www.minsocam.org or GeoscienceWorld

high T (de Koker et al. 2013). Yet it is known that the band gap in LDA calculations is typically too small, up to 40% in several cases (Perdew, 1985). For MgO-periclase, Tran and Blaha (2009) predicted, using LDA, a band gap energy of 4.70 eV compared to the experimental value of 7.83 eV. Anisimov and Kozhevnikov (2005) explained how the one-electron eigenvalues in LDA calculations are Kohn–Sham energies that do not directly correspond to excitation energies. In theory, such a difference in the energy band gap could significantly alter the energetic properties of MgO under extreme conditions of temperature only (between about 54500 K and 91000 K if the band gap scales to k_BT). In this context, the presence of an electronic contribution in the definition of the Gibbs energy of MgO-SiO_2 melts in the 3000 – 10000 K range as reported by de Koker et al. (2013) is surprising, even if the band gap was reduced upon melting and mixing with SiO_2 in various amounts. This electronic contribution should be taken with care as it could easily be an artifact from the LDA when predicting the band gap of these melts. De La Pierre et al. (2011) studied in detail the performance of 6 functionals in the simulation of the vibrational and dielectric properties of solid forsterite. They concluded that the LDA is the worst performing functional. A direct observation of the imprecision of electronic band gaps from LDA can be found in the work of Cococcioni et al. (2003), which predicts a metallic ground state for solid fayalite, contrary to experimental evidence that indicates an insulating, possibly Mott-Hubbard, behavior.

For these reasons, exploration of the accuracy of GGA-based MD simulations of silicate melts at high P and T seems warranted. Moreover, it is well documented (Hautier et al. 2012) that transition metals such as Fe, Mn and Ni in oxide materials require the use of GGA and other corrections such as the Hubbard parameter (Anisimov et al. 1991) to account for strong correlation of electrons in the d-states (Cococcioni and de Gironcoli, 2005). This will be an issue

Always consult and cite the final, published document. See http://www.minsocam.org or GeoscienceWorld

when trying to extend binary MgO-SiO_2 calculations and compatibly merge them with ternary and higher systems, especially when incorporating iron, the third-most abundant cation in Earth's mantle. Spera et al. (2011) pointed out important differences in thermo-physical properties for liquid $MgSiO_3$ at high *T* and *P* between corrected LDA MD simulations (Stixrude and Karki 2005) and GGA MD simulations (Wan et al. 2007). There are other differences between these two studies (e.g. the Car and Parrinello (1985) scheme vs. the Born and Oppenheimer (1927) approximation), so the difference may not be entirely LDA vs. GGA. Spera et al. (2011) concluded that key experimental measurements are needed to identify the most accurate approach in this specific case.

7. Cautions concerning other aspects of DFT implementation

In this section we consider several additional issues related to the choices and approximations that are adopted by DFT practitioners, specifically as applied to calculating forces for ab initio MD simulation of multicomponent silicate liquids: the choice of exchange-correlation functional, the approximation adopted to parameterize core electron behavior, and the demonstration of convergence with respect to numerical details such as plane-wave basis cut-off and k-point sampling.

7.1 *Functionals*

The selection of an adequate functional to define the exchange-correlation electronic contribution is of course a critical step when using DFT. Computational resource limitations often govern this choice when simulating complex geological systems using AIMD. This explains the popularity of LDA, the cheapest option, allowing longer MD simulations and bigger supercells for given computational resources. However, LDA is often not the most accurate

Always consult and cite the final, published document. See http://www.minsocam.org or GeoscienceWorld

747 functional for oxide systems. De La Pierre et al. (2011) reported key studies on this topic and
748 highlighted the importance of introducing a fraction of Hartree-Fock (exact) exchange in hybrid
749 functionals to accurately model calcite, quartz, katoite, and garnets. They also performed DFT
750 calculations for forsterite and confirmed that a hybrid functional such as B3LYP (Becke 1993;
751 Lee et al. 1988; Vosko et al. 1980; Stephens et al. 1994) provides the most accurate results.
752 Kotomin et al. (2008) concurred that B3LYP is needed to predict correct band gaps of
753 perovskites, while Strassner and Taige (2005) concluded that a hybrid functional is required for
754 accurate representation of compounds containing transition metals.

755 An efficient and popular choice of hybrid functional is the Hubbard U correction. LDA+U and
756 GGA+U methods, following the work of Anisimov et al. (1991, 1997), can improve the ability of
757 DFT to quantitatively (and even, sometimes, qualitatively) reproduce experimental observations.
758 This approach was applied, for example, by Stackhouse et al. (2010) to study the high-pressure
759 properties of fayalite. They showed that iteration between predicted thermo-physical properties
760 and available experimental data is required to set the value of the U parameter. As for the LDA
761 pressure correction, there is no physical justification to assume that the U parameter is
762 independent of the chemical environment and structure of the considered phase. Therefore, it is
763 not clear how the U parameter should be treated across variable compositions when studying
764 silicate melts under pressure. Also, without any prior knowledge about the physico-chemical
765 behavior of the considered phase obtained from laboratory data, it is not possible to parameterize
766 this empirical correction. Stackhouse et al. (2010) also concluded that the mixed success of the
767 GGA+U approach when studying fayalite justifies the continued development of more exact
768 methods such as Quantum Monte Carlo (Foulkes et al. 2001).

769 7.2 Core electrons

Always consult and cite the final, published document. See http://www.minsocam.org or GeoscienceWorld

Practical DFT generally does not compute the density of all electrons in a system self-consistently. The rapidly oscillating wavefunctions close to atomic nuclei make all-electron calculations very expensive, and at the same time efficient shielding of closed-shell core electrons typically reduces their influence over chemical bonding behavior. So explicit calculation of their electron density is replaced by simplified effective contributions. The most popular methods are pseudo-potential and projector augmented wave (PAW) approaches. Note that PAW methods are built from ultra-soft pseudo-potentials. This in each case, a parameterization is required, as detailed by Jollet et al. (2014). This should be aimed not at fitting empirical data but at converging to the all-electron result. All-electron calculations, however are rarely available for system chemical environments and pressures relevant to multicomponent silicate liquids in planetary mantles. The objective procedure proposed by Lejaeghere et al. (2013) is used in this case to quantify the error of a given pseudo-potential compared to all-electron calculations. In this method, the integrated Birch-Murnaghan EOS (i.e. *E(V)* curve) is fit both to pseudo-potential and all-electron DFT results spanning a volume range ΔV; the difference between these fits is $\Delta E(V)$, and the error is expressed by $\Delta = \sqrt{\int \Delta E^2(V)\, dV \Big/ \Delta V}$. This transferability test is typically performed for elements and binary cubic compounds and will provide sensible results for materials that follow the Birch-Murnaghan EOS only. In some plane wave codes such as VASP (Kresse and Furthmüller, 1996a, b; Kresse and Hafner, 1993, 1994), the user cannot evaluate the impact of these parameters on the precision of results since they cannot be freely modified as in more flexible codes like ABINIT (Gonze et al. 2009), SIESTA (Soler et al. 2002), or CASTEP (Clark et al. 2005). Of course, the parameterization of pseudo-potentials is a difficult task which requires expertise in electronic structure theory. Even thought geoscientists should not be required to play with these parameters

Always consult and cite the final, published document. See http://www.minsocam.org or GeoscienceWorld

when modeling systems using DFT, there should be efforts to generate benchmark testing for evaluating the transferability and accuracy of these pseudo-potentials using structures and conditions more suited for geological and planetary applications, i.e. more chemically-rich systems subjected to high pressure.

At high *P*, the pseudo-potential cutoff radius can affect the accuracy of calculations. Correa et al. (2006) show the impact of cutoff radius on total energy of liquid, diamond and BC8 carbon phases in AIMD simulations using GGA and norm-conserving pseudo-potentials to describe core electrons. A change of pseudo-potential cutoff radius from 0.74Å to 0.60Å at very high *P* significantly alters the total energy of carbon structures, decreasing the inferred melting point of carbon by 200 K at 1000 GPa. At standard *P* and *T* the single bond length for carbon in diamond is ~1.54 Å (Occelli et al. 2003). This is close to the onset of core overlap at 1.48 Å with the pseudo-potential cutoff radius of Correa et al. (2006). The single bond length of carbon in diamond decreases to about 1.19 Å at 1000 GPa according to the Vinet EOS of Occelli et al. (2003), again close to the 1.2 Å overlap threshold for the high-*P* cutoff radius of Correa et al. (2006). The sensitivity of very high-*P* DFT calculations to pseudo-potential cutoff radius reflects the inability of the pseudo-potential functional form to extrapolate the "exact" orbital wave functions below the radius cutoff. In the case of norm-conserving pseudo-potentials, the core overlap violates the norm-conserving condition, so that integrated charge per orbital deviates from one electron. This is a serious error since these pseudo-potentials rely on norm conservation to guarantee the correct logarithmic eigenvalue derivative that ensures good transferability. For ultra-soft pseudo-potentials, the consequence of overlap is much less severe as they rely on augmentation charge and multiple projectors. However to our knowledge there is no study that attempts to quantify this transferability error as a function of pressure. This emphasizes the

Always consult and cite the final, published document. See http://www.minsocam.org or GeoscienceWorld

importance of customizing the pseudo-potential benchmark tests for geological applications in order to ensure the highest achievable precision of the DFT in these equilibrium conditions.

As another example, Karki et al. (2007) applied the $3s^2 3p^2$ valence state reference and a cutoff radius of 0.82 Å for silicon atoms in silica liquid. With the ultra-soft pseudo-potential of oxygen (0.82 Å and $2s^2 2p^4$), a minimal Si-O distance of 1.64 Å can be studied without electronic core overlap. This is virtually equal to the AIMD simulation value obtained for pure liquid silica by these authors. In another AIMD study on Mg_2SiO_4 liquid, de Koker et al. (2008) applied an ultra-soft pseudo-potential for Si having 0.95 Å cutoff radius and $3s^2 3p^2$ reference valence state, with the same oxygen pseudo-potential. The predicted Si-O distance (≈1.63 Å) in their simulations is smaller than the distance (1.77 Å) for onset of electronic core overlapping based on the reported cutoff radii. The Si-O bond-length alone, although virtually equal in both simulations, cannot warrant the exact same transferability precision of these two distinct pseudo-potentials when evaluating any thermo-physical property. In this context, it should be explained and quantified whether ultra-soft pseudo-potential calculations can be applied to interactions requiring core overlap, and importantly whether errors will become worse as *P* increases and bonds get shorter.

7.3 *Numerical precision*

Finally, a convergence test with respect to the selected basis set (i.e plane-wave cut-off) and the density of k-point sampling over the Brillouin-zone must be performed for at conditions specific enough to each calculation in a study to provide a quantified estimate of errors due to these simplifications for that calculation in particular. An example of such a careful convergence test is presented by de Koker et al. (2008) for Mg_2SiO_4 liquid. They found in this case an uncertainty of 8.8 kJ/mol on the internal energy and 1.5 GPa on the total pressure of their AIMD simulations. In other words, they provide not only the selected cut-off radius and k-point density but also the

Always consult and cite the final, published document. See http://www.minsocam.org or GeoscienceWorld

residual uncertainty they tolerate at the chosen level of convergence. It should be pointed out here that this convergence test cannot be replaced by selection of a different exchange-correlation function. A badly converged simulation with respect to these parameters cannot provide accurate results even with an accurate functional such as B3LYP.

8. Cautions concerning van der Waals interactions

Another important consideration regarding conventional DFT based simulations is that they cannot account for van der Waals interactions arising from mutual dynamical polarization of the interacting atoms, as highlighted by Vuilleumier et al. (2009). Langreth et al. (2005) introduce van der Waals DFT to correct this problem. More recent and widespread adoptions of the so-called DFT-D method to overcome these limitations are presented by Grimme (2006) and Tkatchenko et al. (2009) respectively.

However, classical interatomic force-field potentials are another possible solution to this problem. In this approach, an analytical function describing energetic interaction between atoms as a function of their inter-distance r_{ij} is proposed based on fundamental physics theories. In the specific case of condensed silicate phases, a standard approach to the interionic potential ϕ_{ij} includes Coulomb, repulsive and attractive terms, e.g., (Bukowinski and Akber-Knutson, 2005):

$$\phi_{ij} = \frac{I_i I_j}{r_{ij}} + b_{ij} \exp\left(\frac{-r_{ij}}{\rho_{ij}}\right) - \frac{c_{ij}}{r_{ij}^6} \quad (5)$$

Where I_i is the charge on the i^{th} ion, and b_{ij}, ρ_{ij}, and c_{ij} are parameters that describe a given pair of atoms. In silicate melts, Van der Waals forces are generally introduced in the description of U (c_{ij} parameters) for some (Guillot and Sator, 2007; Lacks et al. 2007) or all interionic interactions

Always consult and cite the final, published document. See http://www.minsocam.org or GeoscienceWorld

(Matsui, 1998). Empirical parameters of such a classical interionic potential for silicate systems are typically obtained by reproducing experimental data for both solid and liquid phases. Hence, classical interatomic potentials can only be used if enough thermo-physical data are available and that their predictive abilities depend on the physical complexity of the functional form used to describe the energetics of the considered structure.

Moreover, a pairwise-type potential is only an effective description of the energetic interactions in condensed phases, since many-body interactions may be present. These higher-order interactions should logically be accounted for in a rigorous analytical treatment of condensed matter energetics. For example, there should be an energetic perturbation induced by a third ion on a given ionic pair (influence of the chemical environment). Salanne et al. (2012) proposed a general formalism for improving interionic potentials like Equation 5, to account for the most important many-body effects in the overlap repulsion component and the polarization part of their potential, based on the aspherical ion model (Aguado et al. 2003; Aguado and Madden, 2004; Jahn and Madden, 2007). This complex functional form is parameterized by the force-fitting or force-matching method (Laio et al. 2000), and only DFT stress and force calculations are used as input data. These authors also highlighted the conundrum induced by this procedure: as there is no dynamical polarization in conventional DFT calculations, results of these simulations do not constrain the dispersion interaction parameters of their functional, which are therefore not included in the fitting procedure. However, dispersive terms are introduced in their functional a posteriori based on other considerations (Salanne et al. 2012).

The approach of Salanne et al. (2012) is a clear improvement over the conventional classical fitting of empirical pairwise interionic potentials to a limited set of experimental data. Use of DFT results spanning a range of *P, T,* and atomic configurations leads to a more transferable

Always consult and cite the final, published document. See http://www.minsocam.org or GeoscienceWorld

potential and encompasses energetic contributions not explicitly defined in their functional via correlated terms. There are still important limitations to such an approach. First, the original force-fitting approach proposed by Laio et al. (2000) was intended for the parameterization of interionic potentials for a specific set of (P, T) equilibrium conditions only and may not be fully transferable to other equilibrium conditions. Even the more complex many-body interionic functional form does not explicitly represent important phenomena such as metallization of ionic interactions at high T and P (de Koker and Stixrude, 2009). Without an explicit treatment of the effect of P on the electronic density of states in these interionic potentials, one can only hope to fold these effects into correlated terms for a given set of (P, T) conditions. Determining a single set of interionic parameters for a range of T, P and composition will inevitably result in a loss of precision, as observed by Salanne et al. (2012) for silica-rich melts.

9. Implications

We have presented several limitations of current MD simulations, inherent to the technique (kinetic limitations, limited computing resources, etc.) or to our limited knowledge of atomistic phenomena underlying the evolution of many-body interactions in silicate solutions as a function of T, P and composition. These constructive criticisms are not intended to discourage the reader from applying classical or ab initio MD simulation methods to Earth science problems. Instead, the intent is to stimulate interdisciplinary discussions among physicists and geochemists, to refine our fundamental understanding of silicate melts, solids and glasses. Another goal of the present communication is to provide scientists unfamiliar with the detail of quantum simulation methods with a better appreciation of the potential errors and uncertainties.

Always consult and cite the final, published document. See http://www.minsocam.org or GeoscienceWorld

For the MD simulation expert, this work highlights that many suspicions about the robustness and statistical significance of their work could be allayed simply by more systematic publication of raw simulation data. We would encourage the scientific community to:

1. Present all raw simulation data in appendices or online supplements in order to allow data post-treatment as well as a precise evaluation of the error/uncertainty.
2. Provide the finite-size and time-equilibration data of each simulation.
3. In the case of AIMD simulations, provide the results of the convergence test with respect to the basis set and the k-points for Brillouin zone sampling in terms of stress and force errors.
4. Evaluate instantaneous heat capacity and thermal expansion, when possible, from the variance of the statistical ensemble for comparison to derivatives of fitted thermodynamic models, to quantify the ability of the simulation to span the entire partition function.
5. Study the impact of the initial configuration on the resulting equilibrium state, especially for systems containing miscibility gaps, and including both ordered and disordered initial states. This would ensure that MD simulation parameters used for imposed equilibrium conditions allow the exploration of the true equilibrium state.
6. Design a series of MD simulations to quantifiably observe the evolution of the SRO.

For the experimentalist, we highlight information that ought to be developed in collaboration with MD simulation experts:

1. Provide experiments, such as diffuse X-ray scattering and nuclear magnetic resonance spectroscopy, to quantify the 2NN pair fraction environment in silicate melts, solids and glasses, for validation of current MD simulations and development of future methods.

Always consult and cite the final, published document. See http://www.minsocam.org or GeoscienceWorld

925 2. Target equilibrium conditions of temperature, pressure and composition of fundamental
926 importance for the improvement of physical theories of silicate solutions.

927 For the theoretician, the goals highlighted by this work are:

928 1. Incorporate self-consistent thermo-physical data obtained from MD simulations in
929 classical thermodynamic models to see if they allow accurate prediction of complex
930 phase equilibria for which experimental data are available. This will serve to validate or
931 falsify some of the suspicions raised here.
932 2. Use both simulations and experiments to test new approaches to linking molar volume,
933 internal energy, configurational entropy, and the microscopic internal configuration of
934 melts, to improve predictive abilities of classical thermodynamic models.
935 3. Quantify the importance of Van der Waals forces in silicate melts, perhaps using classical
936 interatomic potentials, to judge if they limit accuracy of AIMD simulations.
937 4. Parameterize more robust interionic potentials that account for many-body interactions.
938

939 **Reference list**

940 Adam, G., and Gibbs, J.H. (1965) On the temperature dependence of cooperative relaxation
941 properties in glass-forming liquids. The Journal of Chemical Physics, 43, 139-146.
942 Agee, C.B. (1998) Crystal-liquid density inversions in terrestrial and lunar magmas. Physics of
943 the Earth and Planetary Interiors, 107, 63-74.
944 Aguado, A., and Madden, P.A. (2004) Fully transferable interatomic potentials for large-scale
945 computer simulations of simple metal oxides: Application to MgO. Physical Review B, 70,
946 245103.

Always consult and cite the final, published document. See http://www.minsocam.org or GeoscienceWorld

947 Aguado, A., Bernasconi, L., Jahn, S., and Madden, P.A. (2003) Multipoles and interaction
948 potentials in ionic materials from planewave-DFT calculations. Faraday Discussions, 124,
949 171-184.
950 Akaogi, M., and Navrotsky, A. (1984) The quartz-coesite-stishovite transformations: new
951 calorimetric measurements and calculation of phase diagrams. Physics of the Earth and
952 Planetary Interiors, 36, 124-134.
953 Alder, B.J. (1964) Studies in molecular dynamics. III. A mixture of hard spheres. The Journal of
954 Chemical Physics, 40, 2724-2730.
955 Alfredsson, M., Brodholt, J.P., Wilson, P.B., Price, G.D., Cora, F., Calleja, M., Bruin, R.,
956 Blanshard, L.J., and Tyer, R.P. (2005) Structural and magnetic phase transitions in simple
957 oxides using hybrid functionals. Molecular Simulation, 31, 367-377.
958 Anisimov, V.I., and Kozhevnikov, A.V. (2005) Transition state method and Wannier functions.
959 Physical Review B, 72, 075125.
960 Anisimov, V.I., Zaanen, J., and Andersen, O.K. (1991) Band theory and Mott insulators:
961 Hubbard *U* instead of Stoner *I*. Physical Review B, 44, 943-954.
962 Anisimov, V. I., Aryasetiawan, F., and Lichtenstein, A. I. (1997) First-principles calculations of
963 the electronic structure and spectra of strongly correlated systems: the LDA + *U* method.
964 Journal of Physics: Condensed Matter, 9, 767-808.
965 Asimow, P.D., and Ahrens, T.J. (2010) Shock compression of liquid silicates to 125 GPa: The
966 anorthite-diopside join. Journal of Geophysical Research: Solid Earth, 115, B10209.
967 Bale, C.W., Belisle, E., Chartrand, P., Decterov, S.A., Eriksson, G., Hack, K., Jung, I.H., Kang,
968 Y.B., Melancon, J., Pelton, A.D., Robelin, C., and Petersen, S. (2009) FactSage
969 thermochemical software and databases - recent developments. CALPHAD, 33, 295-311.

Always consult and cite the final, published document. See http://www.minsocam.org or GeoscienceWorld

970 Baroni, S., de Gironcoli, S., Dal Corso, A., and Giannozzi, P. (2001) Phonons and related crystal
971 properties from density-functional perturbation theory. Review of Modern Physics, 73, 515-
972 562.
973 Becke, A.D. (1993) Density-functional thermochemistry. III. The role of exact exchange. The
974 Journal of Chemical Physics, 98, 5648-5652.
975 Bolmatov, D., Brazhkin, V.V., and Trachenko, K. (2012) The phonon theory of liquid
976 thermodynamics. Scientific Reports, 2, srep00421-1 srep00421-6.
977 Born, M., and Huang, K. (1969) Dynamical Theory of Crystal Lattices, Oxford University Press.
978 Born, M., and Oppenheimer, R. (1927) Zur Quantentheorie der Molekeln (in German). Annalen
979 der Physik, 84, p. 457-484.
980 Brady, J.B. (2013) Diffusion Data for Silicate Minerals, Glasses, and Liquids, in Mineral Physics
981 & Crystallography: A Handbook of Physical Constants. American Geophysical Union, 269-
982 290.
983 Bukowinski, M.S.T., and Akber-Knutson, S. (2005) The Role of Theoretical Mineral Physics in
984 Modeling the Earth's Interior, Earth's Deep Mantle: Structure, Composition, and Evolution.
985 American Geophysical Union, 137-163.
986 Cao, W., Chang, Y.A., Zhu, J., Chen, S., and Oates, W.A. (2007) Thermodynamic modeling of
987 the Cu-Ag-Au system using the cluster/site approximation. Intermetallics, 15, 1438-1446.
988 Car, R., and Parrinello, M. (1985) Unified approach for molecular dynamics and density-
989 functional theory. Physical Review Letters, 55, 2471-2474.
990 Ceperley, D.M., and Alder, B.J. (1980) Ground state of the electron gas by a stochastic method.
991 Physical Review Letters, 45, 566-569.

Always consult and cite the final, published document. See http://www.minsocam.org or GeoscienceWorld

992 Chamberlin, L., Beckett, J.R., and Stolper, E. (1994) Pd-oxide equilibration: a new experimental
993 method for the direct determination of oxide activities in melts and minerals. Contributions to
994 Mineralogy and Petrology, 116, 169-181.
995 Clark, S.J., Segall, M.D., Pickard, C.J., Hasnip, P.J., Probert, M.I.J., Refson, K., and Payne, M.C.
996 (2005) First principles methods using CASTEP. Zeitschrift für Kristallographie, 220, 567-
997 570.
998 Clemens, J.D., and Petford, N. (1999) Granitic melt viscosity and silicic magma dynamics in
999 contrasting tectonic settings. Journal of the Geological Society 156, 1057-1060.
1000 Cococcioni, M., Dal Corso, A., and de Gironcoli, S. (2003) Structural, electronic, and magnetic
1001 properties of Fe_2SiO_4 fayalite: Comparison of LDA and GGA results. Physical Review B,
1002 67, 094106.
1003 Cococcioni, M., and de Gironcoli, S. (2005) Linear response approach to the calculation of the
1004 effective interaction parameters in the LDA+U method. Physical Review B 71, 035105.
1005 Correa, A.A., Bonev, S.A., and Galli, G. (2006) Carbon under extreme conditions: Phase
1006 boundaries and electronic properties from first-principles theory. Proceedings of the National
1007 Academy of Sciences of the United States of America, 103, 1204-1208.
1008 Dalton, J.A., and Presnall, D.C. (1997) No liquid immiscibility in the system $MgSiO_3$-SiO_2 at 5.0
1009 GPa. Geochimica et Cosmochimica Acta, 61, 2367-2373.
1010 Dasgupta, R., and Hirschmann, M.M. (2006) Melting induced extraction of C–O–H volatiles at
1011 mid-ocean ridges. Geochimica et Cosmochimica Acta, 70, A127.
1012 Davies, G.F. (1973) Quasi-harmonic finite strain equations of state of solids. Journal of Physics
1013 and Chemistry of Solids, 34, 1417-1429.

Always consult and cite the final, published document. See http://www.minsocam.org or GeoscienceWorld

Davies, G.F. (2006) Early mantle dynamics: Depletion, plates and a revised cooling history. Geochimica et Cosmochimica Acta, 70, A132.

Davies, G.F. (2008) Episodic layering of the early mantle by the 'basalt barrier' mechanism. Earth and Planetary Science Letters, 275, 382-392.

de Koker, N., and Stixrude, L. (2009) Self-consistent thermodynamic description of silicate liquids, with application to shock melting of MgO periclase and $MgSiO_3$ perovskite. Geophysical Journal International, 178, 162-179.

de Koker, N.P., Stixrude, L., and Karki, B.B. (2008) Thermodynamics, structure, dynamics, and freezing of Mg_2SiO_4 liquid at high pressure. Geochimica et Cosmochima Acta, 72, 1427-1441.

de Koker, N., Karki, B.B., and Stixrude, L. (2013) Thermodynamics of the MgO–SiO_2 liquid system in Earth's lowermost mantle from first principles. Earth and Planetary Science Letters, 361, 58-63.

de La Pierre, M., Orlando, R., Maschio, L., Doll, K., Ugliengo, P., and Dovesi, R. (2011) Performance of six functionals (LDA, PBE, PBESOL, B3LYP, PBE0, and WC1LYP) in the simulation of vibrational and dielectric properties of crystalline compounds. The case of forsterite Mg_2SiO_4. Journal of Computional Chemistry, 32, 1775-1784.

Del Gaudio, P., and Behrens, H. (2009) An experimental study on the pressure dependence of viscosity in silicate melts. The Journal of Chemical Physics, 131, 044504.

Dingwell, D.B. (1996) Volcanic Dilemma--Flow or Blow? Science, 273, 1054-1055.

Dingwell, D.B. (1998) Melt viscosity and diffusion under elevated pressures. Reviews in Mineralogy and Geochemistry, 37, 397-424.

Always consult and cite the final, published document. See http://www.minsocam.org or GeoscienceWorld

Dyer, P.J., and Cummings, P.T. (2006) Hydrogen bonding and induced dipole moments in water: predictions from the Gaussian charge polarizable model and Car-Parrinello molecular dynamics. The Journal of Chemical Physics, 125, 144519.

Dyre, J.C., Hechsher, T., and Niss, K. (2009) A brief critique of the Adam–Gibbs entropy model. Journal of Non-Crystalline Solids, 355, 624-627.

Evans, D.J., and Holian, B.L. (1985) The Nose–Hoover thermostat. The Journal of Chemical Physics, 83, 4069-4074.

Evans, R.L., Hirth, G., Baba, K., Forsyth, D., Chave, A., and Mackie, R. (2005) Geophysical evidence from the MELT area for compositional controls on oceanic plates. Nature, 437, 249-252.

Faul, U.H., and Scott, D. (2006) Grain growth in partially molten olivine aggregates. Contributions to Mineralogy and Petrology, 151, 101-111.

Faul, U.H., Toomey, D.R., and Waff, H.S. (1994) Intergranular basaltic melt is distributed in thin, elongated inclusions. Geophysical Research Letters, 21, 29-32.

Fei, Y., Saxena, S.K., and Navrotsky, A. (1990) Internally consistent thermodynamic data and equilibrium phase relations for compounds in the system MgO-SiO_2 at high pressure and high temperature. Journal of Geophysical Research: Solid Earth, 95, 6915-6928.

Forsyth, D.W. (1996) Partial melting beneath a Mid-Atlantic Ridge Segment detected by teleseismic PKP delays. Geophysical Research Letters, 23, 463-466.

Foulkes, W.M.C., Mitas, L., Needs, R.J., and Rajagopal, G. (2001) Quantum Monte Carlo simulations of solids. Reviews of Modern Physics, 73, 33-83.

Franzblau, M.C., and Gordon, R.B. (1967) The order-disorder transformation in Cu_3Au at high pressure. Journal of Applied Physics 38, 103-110.

Always consult and cite the final, published document. See http://www.minsocam.org or GeoscienceWorld

1059 Fultz, B. (2010) Vibrational thermodynamics of materials. Progress in Materials Science. 55,
1060 247-352.
1061 Garrity, K.F., Bennett, J.W., Rabe, K.M., and Vanderbilt, D. (2014) Pseudopotentials for high-
1062 throughput DFT calculations. Computational Materials Science, 81, 446-452.
1063 Ghiorso, M. (1985) Chemical mass transfer in magmatic processes. Contributions to Mineralogy
1064 and Petrology, 90, 107-120.
1065 Ghiorso, M.S., and Spera, F.J. (2010) Large scale simulations. Reviews in Mineralogy and
1066 Geochemistry, 71, 437-463.
1067 Ghiorso, M.S., Hirschmann, M.M., Reiners, P.W., and Kress, V.C. (2002) The pMELTS: A
1068 revision of MELTS for improved calculation of phase relations and major element
1069 partitioning related to partial melting of the mantle to 3 GPa. Geochemistry, Geophysics,
1070 Geosystems, 3, 1-35.
1071 Ghosh, D.B., and Karki, B.B. (2011) Diffusion and viscosity of Mg_2SiO_4 liquid at high pressure
1072 from first-principles simulations. Geochimica et Cosmochimica Acta, 75, 4591-4600.
1073 Gonze, X., Amadon, B., Anglade, P.M., Beuken, J.M., Bottin, F., Boulanger, P., Bruneval, F.,
1074 Caliste, D., Caracas, R., Côté, M., and others (2009) ABINIT: First-principles approach to
1075 material and nanosystem properties. Computer Physics Communications, 180, 2582-2615.
1076 Grimme, S., (2006) Semiempirical GGA-type density functional constructed with a long-range
1077 dispersion correction. Journal of Computational Chemistry, 27, 1787-1799.
1078 Guillot, B., and Sator, N. (2007) A computer simulation study of natural silicate melts. Part I:
1079 Low pressure properties. Geochimica et Cosmochimica Acta, 71, 1249-1265.
1080 Haas, P., Tran, F., and Blaha, P. (2009) Calculation of the lattice constant of solids with
1081 semilocal functionals. Physical Review B, 79, 085104.

Always consult and cite the final, published document. See http://www.minsocam.org or GeoscienceWorld

Hageman, V.B.M., and Oonk, H.A.J. (1986) Liquid immiscibility in the SiO_2 + MgO, SiO_2 + SrO, SiO_2 + La_2O_3, and SiO_2 + Y_2O_3 systems. Physics and Chemistry of Glasses, 27, 194-198.

Hamann, D.R. (1996) Generalized gradient theory for silica phase transitions. Physical Review Letters, 76, 660-663.

Hautier, G., Ong, S.P., Jain, A., Moore, C.J., and Ceder, G. (2012) Accuracy of density functional theory in predicting formation energies of ternary oxides from binary oxides and its implication on phase stability. Physical Review B, 85, 155208.

Hayoun, M., Pontikis, V., and Winter, C. (1998) Computer simulation study of surface segregation on Cu_3Au. Surface Science, 398, 125-133.

Hicks, D.G., Boehly, T.R., Eggert, J.H., Miller, J.E., Celliers, P.M., and Collins, G.W. (2006) Dissociation of liquid silica at high pressures and temperatures. Physical Review Letters, 97, 025502.

Hirschmann, M.M. (2006) Water, melting, and the deep earth H_2O cycle. Annual Review of Earth and Planetary Sciences, 34, 629-653.

Holm, J.L., Kleppa, O.J., and Westrum E.F.Jr. (1967) Thermodynamics of polymorphic transformations in silica. Thermal properties from 5 to 1070° K and pressure-temperature stability fields for coesite and stishovite. Geochimica et Cosmochimica Acta, 31, 2289-2307.

Horbach, J., Kob, W., Binder, K., and Angell, C.A. (1996) Finite size effects in simulations of glass dynamics. Physical Review E, 54, R5897-R5900.

Hudon, P., Jung, I.-H., and Baker, D.R. (2004) Effect of pressure on liquid-liquid miscibility gaps: A case study of the systems CaO-SiO_2, MgO-SiO_2, and $CaMgSi_2O_6$-SiO_2. Journal of Geophysical Research: Solid Earth, 109, B03207.

Always consult and cite the final, published document. See http://www.minsocam.org or GeoscienceWorld

Hudon, P., Jung, I.-H., and Baker, D.R. (2005) Experimental investigation and optimization of thermodynamic properties and phase diagrams in the systems CaO-SiO_2, MgO-SiO_2, $CaMgSi_2O_6$-SiO_2, and $CaMgSi_2O_6$-Mg_2SiO_4 to 1.0 GPa. Journal of Petrology, 46, 1859-1880.

Ising, E. (1925) Beitrag zur theorie des ferromagnetismus (in German). Zeitschrift für Physik, 31, 253-258.

Jahn, S., and Madden, P.A. (2007) Modeling Earth materials from crustal to lower mantle conditions: A transferable set of interaction potentials for the CMAS system. Physics of the Earth and Planetary Interiors, 162, 129-139.

Jollet, F., Torrent, M., and Holzwarth, N. (2014) Generation of Projector Augmented-Wave atomic data: A 71 element validated table in the XML format. Computer Physics Communications, 185, 1246-1254.

Kambayashi, S., and Kato, E. (1983) A thermodynamic study of (magnesium oxide + silicon dioxide) by mass spectrometry. The Journal of Chemical Thermodynamics, 15, 701-707.

Kambayashi, S., and Kato, E. (1984) A thermodynamic study of (magnesium oxide + silicon dioxide) by mass spectrometry at 1973 K. The Journal of Chemical Thermodynamics, 16, 241-248.

Karato, S.-i., and Jung, H. (1998) Water, partial melting and the origin of the seismic low velocity and high attenuation zone in the upper mantle. Earth and Planetary Science Letters, 157, 193-207.

Karki, B.B., Stixrude, L., and Wentzcovitch, R.M. (2001) High-pressure elastic properties of major materials of Earth's mantle from first principles. Reviews of Geophysics, 39, 507-534.

Always consult and cite the final, published document. See http://www.minsocam.org or GeoscienceWorld

Karki, B.B., Bhattarai, D., and Stixrude, L. (2006) First-principles calculations of the structural, dynamical, and electronic properties of liquid MgO. Physical Review B, 73, 174208.

Karki, B.B., Bhattarai, D., and Stixrude, L. (2007) First-principles simulations of liquid silica: Structural and dynamical behavior at high pressure. Physical Review B, 76, 104205.

Karki, B.B., Zhang, J., and Stixrude, L. (2013) First principles viscosity and derived models for $MgO\text{-}SiO_2$ melt system at high temperature. Geophysical Research Letters, 40, 94-99.

Kikuchi, R. (1951) A theory of cooperative phenomena. Physical Review, 81, 988-1003.

Klein, E.M., and Langmuir, C.H. (1987) Global correlations of ocean ridge basalt chemistry with axial depth and crustal thickness. Journal of Geophysical Research: Solid Earth, 92 (B8), 8089-8115.

Kotomin, E.A., Zhukovskii, Y.F., Piskunov, S., and Ellis, D.E. (2008) Hybrid DFT calculations of the F centers in cubic ABO_3 perovskites. Journal of Physics: Conference Series, 117, 012019.

Kresse, G., and Furthmüller, J. (1996a) Efficiency of ab-initio total energy calculations for metals and semiconductors using a plane-wave basis set. Computational Materials Science, 6, 15-50.

Kresse, G., and Furthmüller, J. (1996b) Efficient iterative schemes for ab initio total-energy calculations using a plane-wave basis set. Physical Review B, 54, 11169-11186.

Kresse, G., and Hafner, J. (1993) Ab initio molecular dynamics for liquid metals. Physical Review B, 47, 558-561.

Kresse, G., and Hafner, J. (1994) Ab initio molecular-dynamics simulation of the liquid-metal–amorphous-semiconductor transition in germanium. Physical Review B, 49, 14251-14269.

Always consult and cite the final, published document. See http://www.minsocam.org or GeoscienceWorld

1150 Kresse, G., and Joubert, D. (1999) From ultrasoft pseudopotentials to the projector augmented-
1151 wave method. Physical Review B, 59, 1758-1775.
1152 Lacks, D.J., Rear, D.B., and Van Orman, J.A. (2007) Molecular dynamics investigation of
1153 viscosity, chemical diffusivities and partial molar volumes of liquids along the $MgO–SiO_2$
1154 join as functions of pressure. Geochimica et Cosmochimica Acta, 71, 1312-1323.
1155 Lacks, D.J., Goel, G., Bopp, C.J.I.V., Van Orman, J.A., Lesher, C.E., and Lundstrom, C.C.
1156 (2012) Isotope fractionation by thermal diffusion in silicate melts. Physical Review Letters,
1157 108, 065901.
1158 Laio, A., Bernard, S., Chiarotti, G.L., Scandolo, S., and Tosatti, E. (2000) Physics of iron at
1159 Earth's core conditions. Science, 287, 1027-1030.
1160 Lange, R.A., and Carmichael, I.S.E. (1987) Densities of Na_2O-K_2O-CaO-MgO-FeO-Fe_2O_3-
1161 Al_2O_3-TiO_2-SiO_2 liquids: New measurements and derived partial molar properties.
1162 Geochimica et Cosmochimica Acta, 51, 2931-2946.
1163 Langreth, D.C., Dion, M., Rydberg, H., Schröder, E., Hyldgaard, P., and Lundqvist, B.I. (2005)
1164 Van der Waals density functional theory with applications. International Journal of Quantum
1165 Chemistry, 101, 599-610.
1166 Lay, T., Garnero, E.J., and Williams, Q. (2004) Partial melting in a thermo-chemical boundary
1167 layer at the base of the mantle. Physics of the Earth and Planetary Interiors, 146, 441-467.
1168 Lee, B.-J., Shim, J.-H., and Baskes, M.I. (2003) Semiempirical atomic potentials for the fcc
1169 metals Cu, Ag, Au, Ni, Pd, Pt, Al, and Pb based on first and second nearest-neighbor
1170 modified embedded atom method. Physical Review B, 68, 144112.
1171 Lee, C., Yang, W., and Parr, R. G. (1988) Development of the Colle-Salvetti correlation-energy
1172 formula into a functional of the electron density. Physical Review B, 37, 785-789.

Always consult and cite the final, published document. See http://www.minsocam.org or GeoscienceWorld

Lee, C.-T.A., Luffi, P., Plank, T., Dalton, H., and Leeman, W.P. (2009) Constraints on the depths and temperatures of basaltic magma generation on Earth and other terrestrial planets using new thermobarometers for mafic magmas. Earth and Planetary Science Letters, 279, 20-33.

Lehnert, K., Su, Y., Langmuir, C.H., Sarbas, B., and Nohl, U. (2000) A global geochemical database structure for rocks. Geochemistry, Geophysics, Geosystems, 1, 1012.

Lejaeghere, K., Van Speybroeck, V., Van Oost, G., Cottenier, S. (2013) Error estimates for solid-state density-functional theory predictions: An overview by means of the ground-state elemental crystals. Critical Reviews in Solid State and Materials Sciences, 39, 1-24.

Lesher, C.E. (2010) Self-diffusion in silicate melts: Theory, observations and applications to magmatic systems. Reviews in Mineralogy and Geochemistry, 72, 269-309.

Liang, Y. (2003) Kinetics of crystal-melt reaction in partially molten silicates: 1. Grain scale processes. Geochemistry, Geophysics, Geosystems, 4, 1045.

Lundstrom, C.C., Chaussidon, M., Hsui, A.T., Kelemen, P., and Zimmerman, M. (2005) Observations of Li isotopic variations in the Trinity ophiolite: evidence for isotopic fractionation by diffusion during mantle melting. Geochimica et Cosmochimica Acta, 69, 735-751.

Martin, G.B., Ghiorso, M., and Spera, F.J. (2012) Transport properties and equation of state of 1-bar eutectic melt in the system $CaAl_2Si_2O_8$-$CaMgSi_2O_6$ by molecular dynamics simulation. American Mineralogist, 97, 1155-1164.

Matsui, M. (1998) Computational modeling of crystals and liquids in the system Na_2O-CaO-MgO-Al_2O_3-SiO_2, Properties of Earth and Planetary Materials at High Pressure and Temperature. AGU, Washington, DC, 145-151.

Always consult and cite the final, published document. See http://www.minsocam.org or GeoscienceWorld

Matsuno, T., Evans, R.L., Seama, N., and Chave, A.D. (2012) Electromagnetic constraints on a melt region beneath the central Mariana back-arc spreading ridge. Geochemistry, Geophysics, Geosystems, 13, Q10017.

McDonough, W.F., and Sun, S.-s. (1995) The composition of the Earth. Chemical Geology, 120, 223-253.

McKenzie, D. (1984) The generation and compaction of partially molten rock. Journal of Petrology, 25, 713-765.

McKenzie, D. (1985) The extraction of magma from the crust and mantle. Earth and Planetary Science Letters, 74, 81-91.

McQuarrie, D.A. (2000) Statistical Mechanics. University Science Books.

McWilliams, R.S., Spaulding, D.K., Eggert, J.H., Celliers, P.M., Hicks, D.G., Smith, R.F., Collins, G.W., and Jeanloz, R. (2012) Phase transformations and metallization of magnesium oxide at high pressure and temperature. Science, 338, 1330-1333.

Metropolis, N., Rosenbluth, A.W., Rosenbluth, M.N., Teller, A.H., and Teller, E. (1953) Equation of state calculations by fast computing machines. The Journal of Chemical Physics, 21, 1087-1092.

Morgan, N.A., and Spera, F.J., (2001a) Glass transition, structural relaxation, and theories of viscosity: a molecular dynamics study of amorphous $CaAl_2Si_2O_8$. Geochimica et Cosmochimica Acta, 65, 4019-4041.

Morgan, N.A., and Spera, F.J., (2001b) A molecular dynamics study of the glass transition in $CaAl_2Si_2O_8$: Thermodynamics and tracer diffusion. American Mineralogist, 86, 915-926.

Neuville, D.R., and Richet, P. (1991) Viscosity and mixing in molten (Ca, Mg) pyroxenes and garnets. Geochimica et Cosmochimica Acta, 55, 1011-1019.

Always consult and cite the final, published document. See http://www.minsocam.org or GeoscienceWorld

1218 Niu, X., Lehnert, K.A., Williams, J., and Brantley, S.L. (2011) CZChemDB and EarthChem:
1219 Advancing management and access of critical zone geochemical data. Applied
1220 Geochemistry, 26 (Supplement), S108-S111.
1221 Oates, W.A., and Wenzl, H. (1996) The cluster/site approximation for multicomponent solutions
1222 -- A practical alternative to the cluster variation method. Scripta Materiala, 35, 623-627.
1223 Oates, W.A., Zhang, F., Chen, S.L., and Chang, Y.A. (1999) Improved cluster-site
1224 approximation for the entropy of mixing in multicomponent solid solutions. Physical Review
1225 B, 59, 11221-11225.
1226 Occelli, F., Loubeyre, P., and LeToullec, R. (2003) Properties of diamond under hydrostatic
1227 pressures up to 140 GPa. Nature Materials, 2, 151-154.
1228 Okamoto, H., Chakrabarti, D.J., Laughlin, D.E., and Massalski, T.B. (1987) The Au-Cu (gold-
1229 copper) system. Bulletin of Alloy Phase Diagrams, 8, 454-474.
1230 Ol'shanskii, Y.I. (1951) Equilibria of two immiscible liquids in systems of alkaline earth
1231 silicates. Doklady Akademii Nauk SSSR, 76, 93-96.
1232 Pelton, A.D., Degterov, S.A., Eriksson, G., Robelin, C., and Dessureault, Y. (2000) The
1233 modified quasichemical model I - binary solutions. Metallurgical and Materials Transactions
1234 B, 31, 651-659.
1235 Perdew, J.P. (1985) Density functional theory and the band gap problem. International Journal of
1236 Quantum Chemistry, 28, 497-523.
1237 Perdew, J.P., and Wang, Y. (1992) Accurate and simple analytic representation of the electron-
1238 gas correlation energy. Physical Review B, 45, 13244-13249.
1239 Pickard, C.J., and Needs, R.J. (2009) Dense low-coordination phases of lithium. Physical Review
1240 Letters, 102, 146401.

Always consult and cite the final, published document. See http://www.minsocam.org or GeoscienceWorld

Plank, T., and Langmuir, C.H. (1988) An evaluation of the global variations in the major element chemistry of arc basalts. Earth and Planetary Science Letters, 90, 349-370.

Poe, B.T., McMillan, P.F., rubie, D.C., Chakraborty, S., Yarger, J., and Diefenbacher, J. (1997) Silicon and oxygen self-diffusivities in silicate liquids measured to 15 gigapascals and 2800 kelvin. Science, 276, 1245-1248.

Putnis, A. (1996) Quantification of disorder in silicate melts, glasses and crystals using NMR spectroscopy. Physics and Chemistry of Minerals, 23, 247.

Rein, R.H., and Chipman, J. (1965) Activities in the liquid solution SiO_2-CaO-MgO-Al_2O_3 at 1600°. Transactions of the American Institute of Mining, Metallurgical and Petroleum Engineers, 233, 415-425.

Revcolevschi, A. (1976) Cooling-rate determination in splat-cooling of oxides. Journal of Materials Science, 11, 563-565.

Richter, F.M., Davis, A.M., DePaolo, D.J., and Watson, E.B. (2003) Isotope fractionation by chemical diffusion between molten basalt and rhyolite. Geochimica et Cosmochimica Acta, 67, 3905-3923.

Rigden, S.M., Ahrens, T.J., and Stolper, E.M. (1988) Shock compression of molten silicate: Results for a model basaltic composition. Journal of Geophysical Research: Solid earth, 93 (B1), 367-382.

Ringwood, A.E. (1962) A model for the upper mantle. Journal of Geophysical Research, 67, 857-867.

Sakamaki, T., Ohtani, E., Urakawa, S., Suzuki, A., and Katayama, Y. (2009) Measurement of hydrous peridotite magma density at high pressure using the x-ray absorption method. Earth and Planetary Science Letters, 287, 293-297.

Always consult and cite the final, published document. See http://www.minsocam.org or GeoscienceWorld

1264 Sakamaki, T., Ohtani, E., Urakawa, S., Suzuki, A., and Katayama, Y. (2010a) Density of dry
1265 peridotite magma at high pressure using an X-ray absorption method. American
1266 Mineralogist, 95, 144-147.
1267 Sakamaki, T., Ohtani, E., Urakawa, S., Suzuki, A., Katayama, Y., and Zhao, D. (2010b) Density
1268 of high-Ti basalt magma at high pressure and origin of heterogeneities in the lunar mantle.
1269 Earth and Planetary Science Letters, 299, 285-289.
1270 Sakamaki, T., Ohtani, E., Urakawa, S., Terasaki, H., and Katayama, Y. (2011) Density of
1271 carbonated peridotite magma at high pressure using an X-ray absorption method. American
1272 Mineralogist, 96, 553-557.
1273 Saksaengwijit, A., and Heuer, A. (2007) Finite-size effects in silica: a landscape perspective.
1274 Journal of Physics: Condensed Matter, 19, 205143.
1275 Salanne, M., Rotenberg, B., Jahn, S., Vuilleumier, R., Simon, C., and Madden, P.A. (2012)
1276 Including many-body effects in models for ionic liquids. Theoretical Chemistry Accounts,
1277 131, 1143.
1278 Schön, J.C., Pentin, I.V., and Jansen, M. (2006) Ab initio computation of low-temperature phase
1279 diagrams exhibiting miscibility gaps. Physical Chemistry Chemical Physics, 8, 1778-1784.
1280 Schubert, G., Turcotte, D.L., and Olson., P. (2001) Mantle Convection in the Earth and Planets.
1281 Cambridge University Press.
1282 Simon, S., Wilke, M., Chernikov, R., Klemme, S., and Hennet, L. (2013) The influence of
1283 composition on the local structure around yttrium in quenched silicate melts - Insights from
1284 EXAFS. Chemical Geology, 346, 3-13.
1285 Sipp, A., and Richet, P. (2002) Equivalence of volume, enthalpy and viscosity relaxation kinetics
1286 in glass-forming silicate liquids. Journal of Non-Crystalline Solids, 298, 202-212.

Always consult and cite the final, published document. See http://www.minsocam.org or GeoscienceWorld

Soler, J. M., Artacho, E., Gale, J. D., García, A., Junquera, J., Ordejón, P., and Sánchez-Portal, D. (2002) The SIESTA method for ab initio order-N materials simulation. Journal of Physics: Condensed Matter, 14, 2745-2779.

Solomatov, V.S., and Stevenson, D.J. (1993) Suspension in convective layers and style of differentiation of a terrestrial magma ocean. Journal of Geophysical Research: Planets, 98 (E3), 5375-5390.

Soules, T.F., Gilmer, G.H., Matthews, M.J., Stolken, J.S., and Feit, M.D. (2011) Silica molecular dynamic force fields—A practical assessment. Journal of Non-Crystalline Solids, 357, 1564-1573.

Sparks, D.W., and Parmentier, E.M. (1991) Melt extraction from the mantle beneath spreading centers. Earth and Planetary Science Letters, 105, 368-377.

Spaulding, D.K., McWilliams, R.S., Jeanloz, R., Eggert, J.H., Celliers, P.M., Hicks, D.G., Collins, G.W., and Smith, R.F. (2012) Evidence for a phase transition in silicate melt at extreme pressure and temperature conditions. Physical Review Letters, 108, 065701.

Spera, F. J., Ghiorso, M. S., and Nevins, D. (2011) Structure, thermodynamic and transport properties of liquid $MgSiO_3$: Comparison of molecular models and laboratory results. Geochimica et Cosmochimica Acta, 75, 1272-1296.

Stackhouse, S., Stixrude, L., and Karki, B.B. (2010) Determination of the high-pressure properties of fayalite from first-principles calculations. Earth and Planetary Science Letters, 289, 449-456.

Strassner, T., and Taige, M.A. (2005) Evaluation of functionals O3LYP, KMLYP, and MPW1K in comparison to B3LYP for delected transition-metal compounds. Journal of Chemical Theory and Computation, 1, 848-855.

Always consult and cite the final, published document. See http://www.minsocam.org or GeoscienceWorld

Stephens, P.J., Devlin, F.J., Chabalowski, C.F., and Frisch, M.J. (1994) Ab initio calculation of vibrational absorption and circular dichroism spectra using density functional force fields. The Journal of Physical Chemistry, 98, 11623-11627.

Sterten, A., and Maeland, I. (1985) Thermodynamics of molten mixtures of sodium hexafluoroaluminate-aluminum oxide and sodium fluoride-aluminum fluoride. Acta Chemica Scandinavica, A39, 241-257.

Stixrude, L., and Karki, B. (2005) Structure and freezing of $MgSiO_3$ liquid in Earth's lower mantle. Science, 310, 297-299.

Stixrude, L., de Koker, N., Sun, N., Mookherjee, M., and Karki, B.B. (2009) Thermodynamics of silicate liquids in the deep Earth. Earth and Planetary Science Letters, 278, 226-232.

Stolper, E., Walker, D., Hager, B.H., and Hays, J.F. (1981) Melt segregation from partially molten source regions: The importance of melt density and source region size. Journal of Geophysical Research: Solid Earth, 86, 6261-6271.

Sugiyama, K., Shinkai, T., and Waseda, Y. (1996) New ADXD/EDXD spectrometer for determining the structure of melts at high temperature. Science Reports of the Research Institutes, Tohoku University, A42, 231-237.

Tikunoff, D., and Spera, F. (2014) Thermal conductivity of molten and glassy $NaAlSi_3O_8$, $CaMgSi_2O_6$ and Mg_2SiO_4 by non equilibrium molecular dynamics at elevated temperature and pressure: Methods and results. American Mineralogist, in press.

Tkatchenko, A., and Scheffler, M. (2009) Accurate molecular van der Waals interactions from ground-state electron density and free-atom reference data. Physical Review Letters, 102, 073005.

Always consult and cite the final, published document. See http://www.minsocam.org or GeoscienceWorld

Tran, F., and Blaha, P. (2009) Accurate band gaps of semiconductors and insulators with a semilocal exchange-correlation potential. Physical Review Letters, 102, 226401.

Urbain, G., Bottinga, Y., and Richet, P. (1982) Viscosity of liquid silica, silcates, and aluminosilicates. Geochimica et Cosmochimica Acta, 46, 1061-1072.

van de Walle, A., and Ceder, G. (1999) Correcting overbinding in local-density-approximation calculations. Physical Review B, 59, 14992-15001.

Vetere, F., Behrens, H., Schuessler, J.A., Holtz, F., Misiti, V., and Borchers, L. (2008) Viscosity of andesite melts and its implication for magma mixing prior to Unzen 1991–1995 eruption. Journal of Volcanology and Geothermal Research, 175, 208-217.

Vinet, P., Ferrante, J., Rose, J.H., and Smith, J.R. (1987) Compressibility of solids. Journal of Geophysical Research: Solid Earth, 92, 9319-9325.

Vollmayr, K., Kob, W., and Binder, K. (1996) Cooling-rate effects in amorphous silica: A computer-simulation study. Physical Review B, 54, 15808-15827.

von Bargen, N., and Waff, H.S. (1986) Permeabilities, interfacial areas and curvatures of partially molten systems: Results of numerical computations of equilibrium microstructures. Journal of Geophysical Research: Solid Earth, 91, 9261-9276.

Vosko, S.H., Wilk, L., and Nusair, M., (1980) Accurate spin-dependent electron liquid correlation energies for local spin density calculations: A critical analysis. Canadian Journal of Physics, 58, 1200-11.

Vuilleumier, R., Sator, N., and Guillot, B. (2009) Computer modeling of natural silicate melts: What can we learn from ab initio simulations. Geochimica et Cosmochimica Acta, 73, 6313-6339.

Always consult and cite the final, published document. See http://www.minsocam.org or GeoscienceWorld

Wan, J.T.K., Duffy, T.S., Scandolo, S., and Car, R. (2007) First-principles study of density, viscosity, and diffusion coefficients of liquid $MgSiO_3$ at conditions of the Earth's deep mantle. Journal of Geophysical Research, Solid Earth, 112, B03208.

Wentzcovitch, R.M., Yu, Y.G., and Wu, Z. (2010) Thermodynamic properties and phase relations in mantle minerals investigated by first principles quasiharmonic theory. Reviews in Mineralogy and Geochemistry, 71, 59-98.

Whittington, A.G., Bouhifd, M.A., and Richet, P. (2009) Amorphous materials: properties, structure, and durability: The viscosity of hydrous $NaAlSi_3O_8$ and granitic melts: Configurational entropy models. American Mineralogist, 94, 1-16.

Williams, Q., and Garnero, E.J. (1996) Seismic evidence for partial melt at the base of Earth's mantle. Science, 273, 1528-1530.

Wu, P., Eriksson, G., Pelton, A.D., and Blander, M. (1993) Prediction of the thermodynamic properties and phase diagrams of silicate systems -- Evaluation of the FeO-MgO-SiO_2 system. ISIJ International, 33, 26-35.

Yeh, I.-C., and Hummer, G. (2004) System-size dependence of diffusion coefficients and viscosities from molecular dynamics simulations with periodic boundary conditions. The Journal of Physical Chemistry B, 108, 15873-15879.

Zaitsev, A.I., Shelkova, N.E., and Mogutnov, B.M. (2000) Thermodynamics of Na_2O-SiO_2 melts. Inorganic Materials, 36, 529-543.

Zhang, L. (2011) Thermodynamic properties calculation for MgO-SiO_2 liquids using both empirical and first-principles molecular simulations. Physical Chemistry Chemical Physics, 13, 21009-21015.

Always consult and cite the final, published document. See http://www.minsocam.org or GeoscienceWorld

1376 Zhang, Y., and Ni, H. (2010) Diffusion of H, C, and O components in silicate melts. Reviews in
1377 Mineralogy and Geochemistry, 72, 171-225.
1378 Zhang, Y., Ni, H., and Chen, Y. (2010) Diffusion data in silicate melts. Reviews in Mineralogy
1379 and Geochemistry, 72, 311-408.
1380 Zhang, Y., Guo, G., Refson, K., and Zhao, Y. (2004) Finite-size effect at both high and low
1381 temperatures in molecular dynamics calculations of the self-diffusion coefficient and
1382 viscosity of liquid silica. Journal of Physics: Condensed Matter, 16, 9127-9135.
1383

Always consult and cite the final, published document. See http://www.minsocam.org or GeoscienceWorld

1384 Table 1: Evaluation of corrections to internal energy $\Delta U_{emp} = -P_{emp}\left(V_0^{FST} - V_0\right)$ and enthalpy

1385 $\Delta H_{emp} = \Delta U_{emp} + \left(P_{emp}V_0^{FST} - P_0V_0^{FST}\right)$ induced by correction for LDA overbinding using an

1386 empirical pressure shift P_{emp}.

Compo.	V_0 (cm^3/mol)[a]	P_{emp} (GPa)[a]	V_0^{FST} (cm^3/mol)	ΔU_{emp} (J/mol)	ΔH_{emp} (J/mol)
MgO	16.46	1.23	15.91	677	20246
$Mg_{5/6}Si_{1/6}O_{7/6}$	17.92	1.54	16.97	1457	27572
$Mg_{2/3}Si_{1/3}O_{4/3}$	19.47	1.74	18.11	2369	33915
$Mg_{3/5}Si_{2/5}O_{7/5}$	20.10	1.79	18.60	2691	36059
$Mg_{1/2}Si_{1/2}O_{3/2}$	20.90	1.84	19.24	3054	38456
$Mg_{1/3}Si_{2/3}O_{5/3}$	22.50	1.83	20.34	3958	41226
$Mg_{1/4}Si_{3/4}O_{7/4}$	23.38	1.79	21.11	4052	41812
$Mg_{1/6}Si_{5/6}O_{11/6}$	24.33	1.72	21.99	4022	41821
		2.34[b]		*5476*	*56932*
SiO_2	27.80	1.50	24.63	4755	41700

1387 Note(s): The Helmholtz energy function parameterized by de Koker et al. (2013) based on the

1388 finite strain theory is applied to each MgO-SiO_2 melts composition at 3000 K and 0 GPa in order

1389 to evaluate uncorrected volumes V_0^{FST} presented in this table.

1390 [a] Data provided by de Koker et al. (2013)

1391 [b] Predicted thermo-physical properties based on a new P_{emp} estimate (see Figure 5).

Always consult and cite the final, published document. See http://www.minsocam.org or GeoscienceWorld

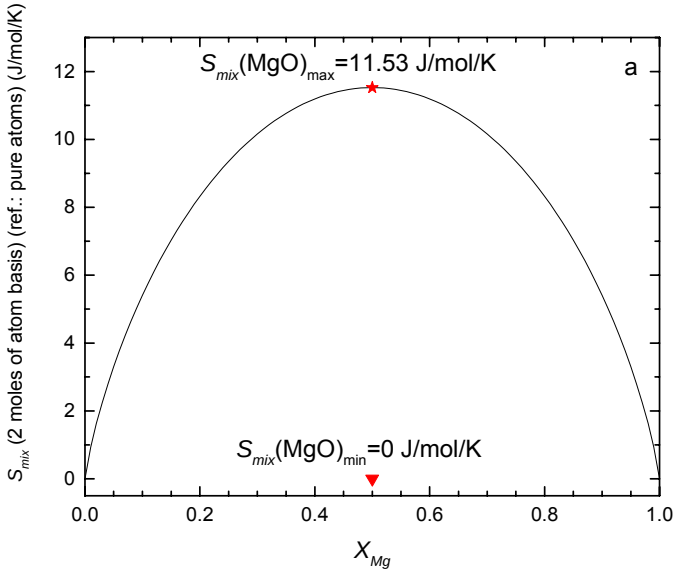

1392

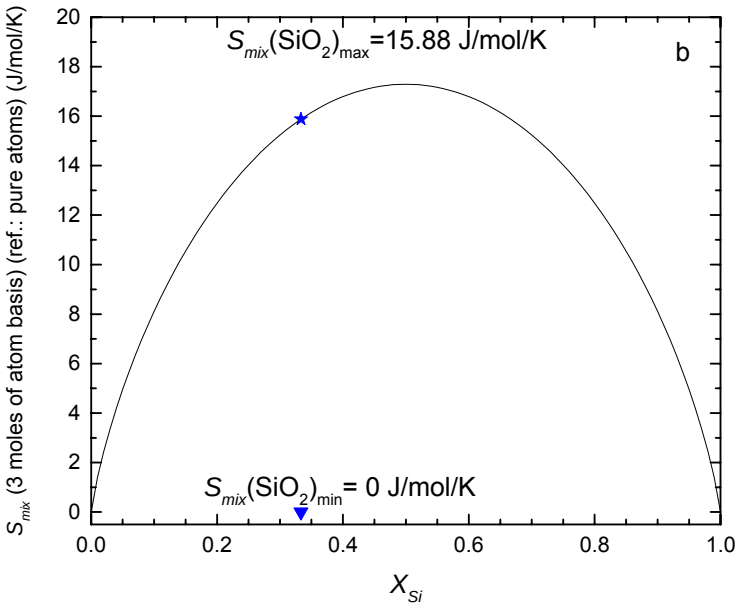

1393

1394 Figure 1: Configurational entropy of mixing, S_{mix}, for the (**a**) Mg-O (2 atom basis) and (**b**) Si-O

1395 (3 atom basis) systems

1396

Always consult and cite the final, published document. See http://www.minsocam.org or GeoscienceWorld

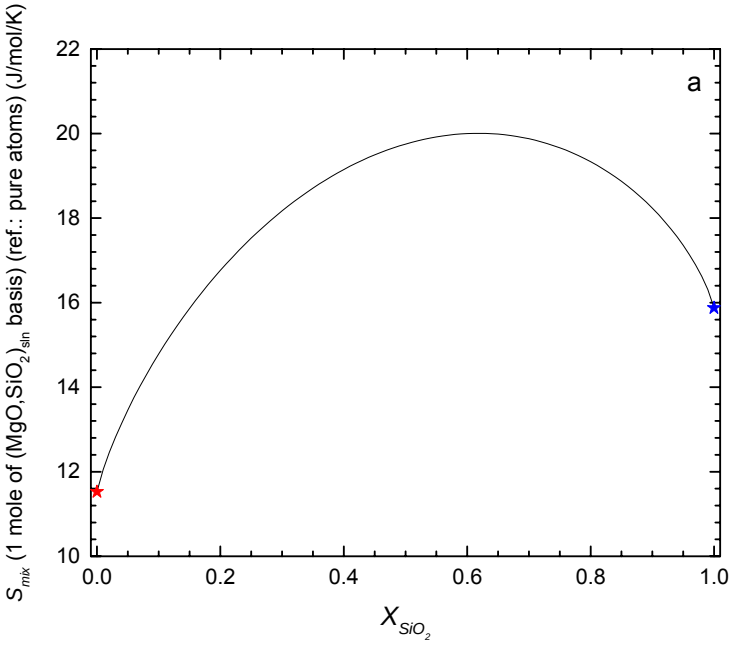

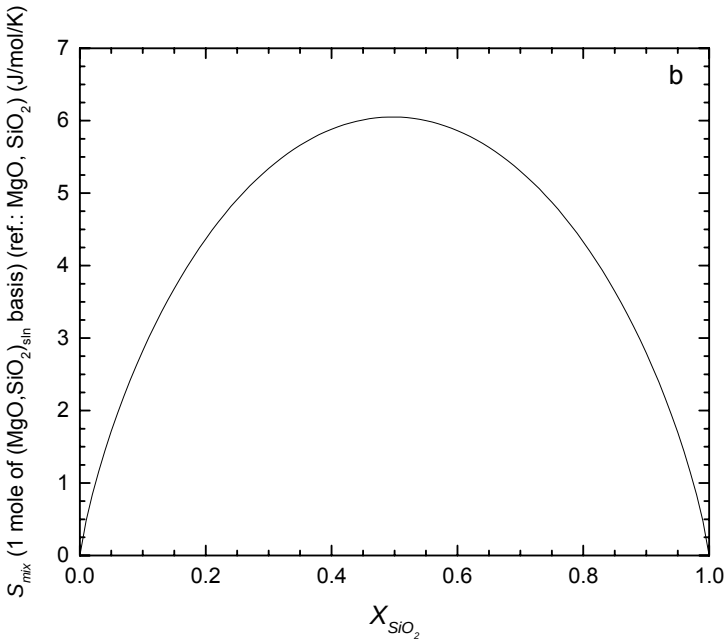

Figure 2: Maximum configurational entropy of mixing, S_{mix}, for the MgO-SiO_2 system referenced to (a) atoms and (b) to MgO and SiO_2 species

Always consult and cite the final, published document. See http://www.minsocam.org or GeoscienceWorld

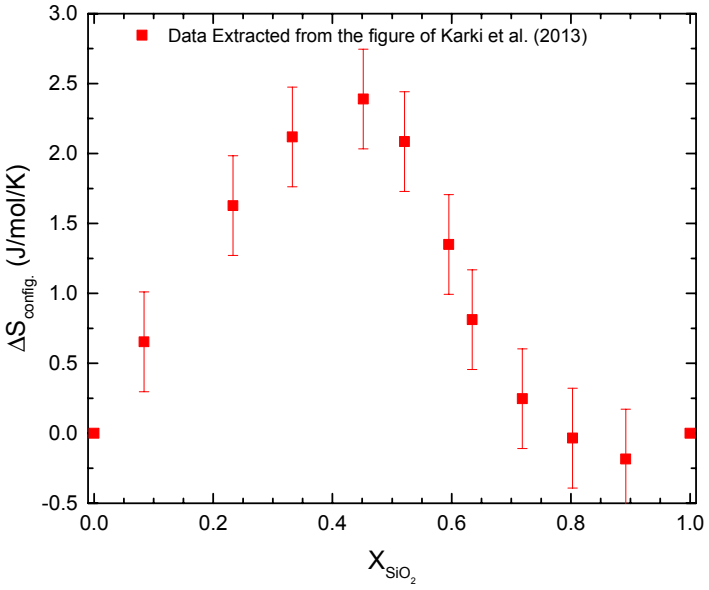

1402

1403 Figure 3: Configurational entropy of mixing, S_{mix}, at 0 GPa for the liquid MgO-SiO_2 system

1404 obtained by applying the Adam-Gibbs theory to represent AIMD viscosity data as presented by

1405 Karki et al. (2013)

1406

Always consult and cite the final, published document. See http://www.minsocam.org or GeoscienceWorld

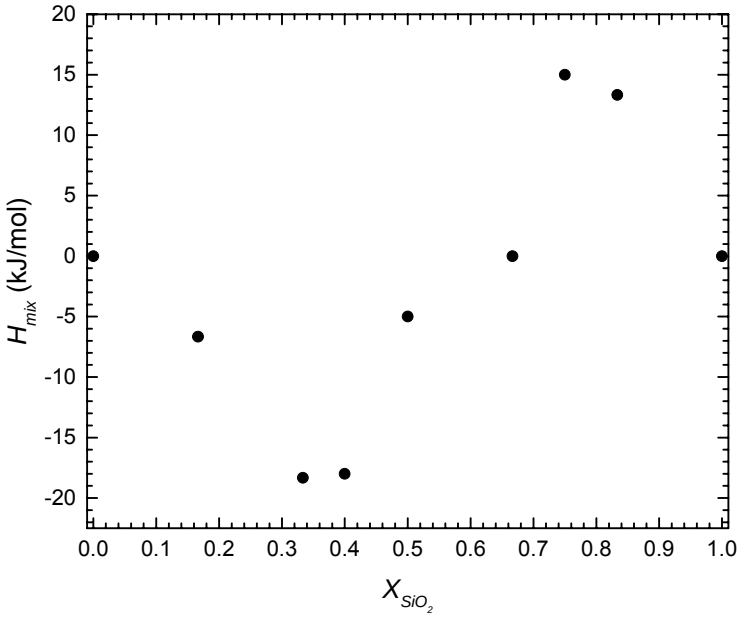

1407

1408 Figure 4: Enthalpy of mixing, H_{mix}, vs X_{SiO_2} at 2000 K and 0 GPa obtained from the raw

1409 appendix data of de Koker et al. (2013).

1410

Always consult and cite the final, published document. See http://www.minsocam.org or GeoscienceWorld

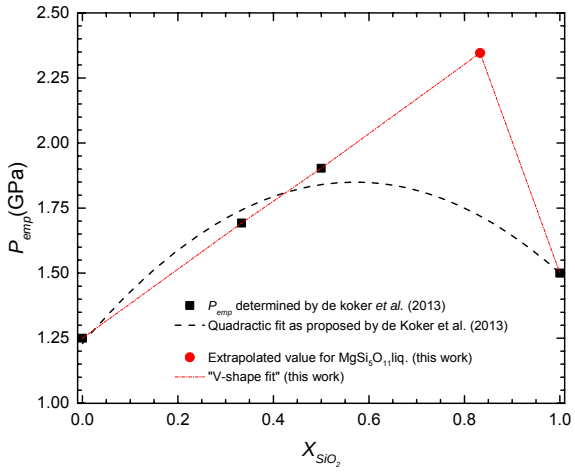

1411

1412 Figure 5: Evaluation of the pressure correction function for systematic overbinding of LDA for
1413 the MgO-SiO_2 system based on computed anchor points where solid phases of known zero-
1414 pressure volume are available (square symbols), from de Koker et al. (2013). The dashed line
1415 represents the quadratic representation of de Koker et al. (2013) while the dashed and dotted line
1416 represents a "V-shape" pressure correction function based on a linear extrapolation of all the
1417 MgO-rich anchor points up to the $MgSi_5O_{11}$ liquid composition as proposed in this work.

1418

Always consult and cite the final, published document. See http://www.minsocam.org or GeoscienceWorld

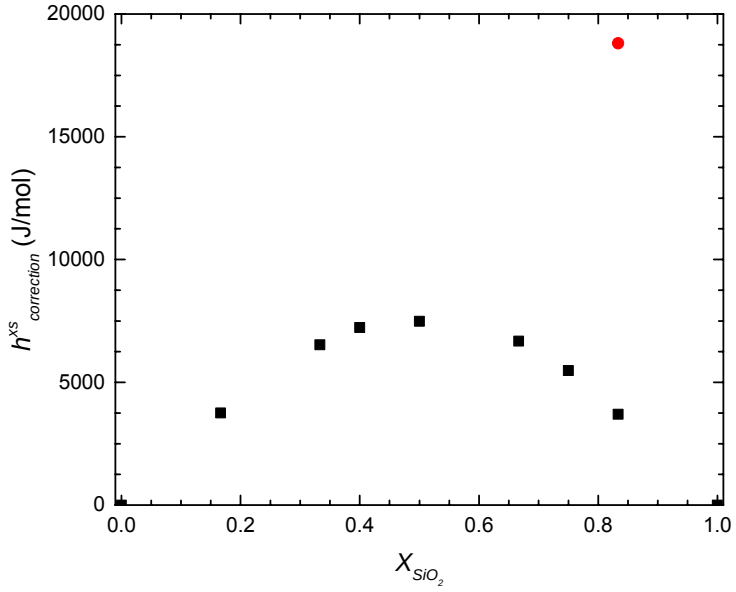

1419

1420 Figure 6: Excess enthalpy correction $h^{xs}_{correction}$ induced by the systematic pressure correction of
1421 LDA calculations as proposed by de Koker et al. (2013) for the MgO-SiO_2 system at 0 GPa and
1422 3000 K. Symbols presented in this figure show the $h^{xs}_{correction}$ correction to be applied using $P_{emp.}$ of
1423 de Koker et al. (2013) (squares) and as proposed in the present work (filled circle).

Always consult and cite the final, published document. See http://www.minsocam.org or GeoscienceWorld

Table 1: Evaluation of corrections to internal energy $\Delta U_{emp} = -P_{emp}\left(V_0^{FST} - V_0\right)$ and enthalpy $\Delta H_{emp} = \Delta U_{emp} + \left(P_{emp}V_0^{FST} - P_0V_0^{FST}\right)$ induced by correction for LDA overbinding using an empirical pressure shift P_{emp}.

Compo.	V_0 (cm^3/mol)[a]	P_{emp} (GPa)[a]	V_0^{FST} (cm^3/mol)	ΔU_{emp} (J/mol)	ΔH_{emp} (J/mol)
MgO	16.46	1.23	15.91	677	20246
$Mg_{5/6}Si_{1/6}O_{7/6}$	17.92	1.54	16.97	1457	27572
$Mg_{2/3}Si_{1/3}O_{4/3}$	19.47	1.74	18.11	2369	33915
$Mg_{3/5}Si_{2/5}O_{7/5}$	20.10	1.79	18.60	2691	36059
$Mg_{1/2}Si_{1/2}O_{3/2}$	20.90	1.84	19.24	3054	38456
$Mg_{1/3}Si_{2/3}O_{5/3}$	22.50	1.83	20.34	3958	41226
$Mg_{1/4}Si_{3/4}O_{7/4}$	23.38	1.79	21.11	4052	41812
$Mg_{1/6}Si_{5/6}O_{11/6}$	24.33	1.72	21.99	4022	41821
		2.34[b]		*5476*	*56932*
SiO_2	27.80	1.50	24.63	4755	41700

Note(s): The Helmholtz energy function parameterized by de Koker et al. (2013) based on the finite strain theory is applied to each MgO-SiO_2 melts composition at 3000 K and 0 GPa in order to evaluate uncorrected volumes V_0^{FST} presented in this table.

[a] Data provided by de Koker et al. (2013)

[b] Predicted thermo-physical properties based on a new P_{emp} estimate (see Fig. 5).